Structural basis for activation of SAGA histone acetyltransferase Gcn5 by partner subunit Ada2

Jian Sun[a], Marcin Paduch[b,1], Sang-Ah Kim[a], Ryan M. Kramer[a,2], Adam F. Barrios[a,3], Vincent Lu[b], Judy Luke[b], Svitlana Usatyuk[b], Anthony A. Kossiakoff[b], and Song Tan[a,4]

[a]Center for Eukaryotic Gene Regulation, Department of Biochemistry and Molecular Biology, The Pennsylvania State University, University Park, PA 16802; and [b]Department of Biochemistry and Molecular Biology, The University of Chicago, IL 60637

Edited by Robert E. Kingston, Massachusetts General Hospital/Harvard Medical School, Boston, MA, and approved August 16, 2018 (received for review March 29, 2018)

The Gcn5 histone acetyltransferase (HAT) subunit of the SAGA transcriptional coactivator complex catalyzes acetylation of histone H3 and H2B N-terminal tails, posttranslational modifications associated with gene activation. Binding of the SAGA subunit partner Ada2 to Gcn5 activates Gcn5's intrinsically weak HAT activity on histone proteins, but the mechanism for this activation by the Ada2 SANT domain has remained elusive. We have employed Fab antibody fragments as crystallization chaperones to determine crystal structures of a yeast Ada2/Gcn5 complex. Our structural and biochemical results indicate that the Ada2 SANT domain does not activate Gcn5's activity by directly affecting histone peptide binding as previously proposed. Instead, the Ada2 SANT domain enhances Gcn5 binding of the enzymatic cosubstrate acetyl-CoA. This finding suggests a mechanism for regulating chromatin modification enzyme activity: controlling binding of the modification cosubstrate instead of the histone substrate.

epigenetics | chromatin biology | histone modification | X-ray crystallography

The acetylation of lysine residues in the histone protein component of chromatin is an important means of regulating gene expression (1–3). The acetyl mark recruits acetyl-lysine binding modules such as the bromodomain found in many gene-regulatory chromatin modification and remodeling enzymes (4, 5). Furthermore, acetylation can neutralize the positive charge of the lysine side chain, leading to destabilization of the nucleosome complex of histone proteins and DNA (2, 6, 7).

Gcn5 is one of the best characterized histone acetyltransferase (HAT) enzymes. Like other members of the Gcn5-related *N*-acetyltransferase family of HAT enzymes, Gcn5 contains a 160-residue catalytic domain necessary for histone acetylation (8). This catalytic domain transfers the acetyl group from acetyl-CoA to the recipient lysine residue on the histone peptide substrate (9). Kinetic studies of the Gcn5 HAT domain have determined that the catalytic mechanism employs an ordered Bi-Bi mechanism with acetyl-CoA binding first, followed by histone peptide binding, and that formation of this ternary complex is required for catalysis (10). Crystallographic and NMR studies of the Gcn5 HAT domain from yeast, human, and *Tetrahymena* provide structural descriptions for acetyl-CoA and histone peptide binding (11–16).

Gcn5 is found in the cell as part of multisubunit gene-regulatory complexes, including the SAGA and variant SAGA complexes (17–21). Whereas Gcn5 acetylates histone H3 weakly on its own and is not able to acetylate histones packaged into nucleosomes, the SAGA complex robustly acetylates nucleosomal histones (22). We and others have previously shown that Gcn5 forms a complex with SAGA subunits Ada2 and Ada3, and that this Ada2/Ada3/Gcn5 complex is necessary and sufficient for SAGA's physiological HAT activity on nucleosomes (23, 24). We also showed that Ada2 activates Gcn5's HAT activity on histone peptides, but Ada3 is required for nucleosomal HAT activity (24).

Deletion analysis of Gcn5 and Ada2 have defined regions required for their protein interaction and for HAT activity (23, 25–27). Approximately 20 residues of Gcn5 immediately following the HAT domain are necessary for Ada2 to bind to Gcn5, and consequently this region (Gcn5 residues 260–280) has been defined as the Ada2 interaction domain (26, 27). The SANT (Swi3, Ada2, N-Cor, and TFIIB) domain of Ada2 plays a critical role in Ada2's interaction with Gcn5, as well as histone and nucleosomal HAT activity by the SAGA complex (27–29). It has been suggested that the SANT domain in Ada2 and other chromatin enzymes functions as a histone tail-binding module to present histone tails for efficient catalysis (28). The SANT domain's structural similarity to the helix-turn-helix DNA-binding domain of Myb transcription factor also suggests the possibility that the Ada2 SANT domain could influence nucleosomal HAT activity by binding nucleosomal DNA (27).

The mechanistic basis for how the Ada2 SANT domain increases Gcn5's catalytic activity has been hampered by the lack of structural information for how Ada2 interacts with Gcn5. We present here crystal structures of the Ada2/Gcn5 complex. The structures show how the SANT and ZZ domains of Ada2 interact with N- and C-terminal extensions to the Gcn5 HAT domain. The Ada2 SANT domain does not appear to act as a

Significance

Regulating gene expression is critical to the normal function of a biological cell, and misregulation of gene expression often leads to a diseased cell. In eukaryotic cells, DNA genetic information is wrapped around histone proteins into chromatin. Modification of histone proteins with the acetyl chemical group (i.e., acetylation) is an important mechanism for activating gene expression. Our biochemical and structural studies of the Gcn5 histone acetyltransferase and its partner protein Ada2 explain how Ada2 activates Gcn5's enzymatic activity without directly contacting the histone substrate, as previously proposed. Instead, Ada2 indirectly influences binding of the enzyme cofactor acetyl-CoA, a mechanism not previously observed for histone modification enzymes.

Author contributions: A.A.K. and S.T. designed research; J.S., R.M.K., and A.F.B. performed research; M.P., S.-A.K., V.L., J.L., S.U., and A.A.K. contributed new reagents/analytic tools; J.S. and S.T. analyzed data; and J.S., M.P., A.A.K., and S.T. wrote the paper.

The authors declare no conflict of interest.

This article is a PNAS Direct Submission.

Data deposition: The atomic coordinates and structure factors have been deposited in the Protein Data Bank, www.wwpdb.org (PDB ID codes 6CW2 and 6CW3).

[1]Present address: Grail, Menlo Park, CA 94402.

[2]Present address: 711th Human Performance Wing, Human Systems Directorate, Battlespace Visualization Branch, Air Force Research Laboratory, Wright Patterson AFB, OH 45305.

[3]Present address: DesigneRx Pharmaceuticals, Vacaville, CA 95688.

[4]To whom correspondence should be addressed. Email: sxt30@psu.edu.

This article contains supporting information online at www.pnas.org/lookup/suppl/doi:10.1073/pnas.1805343115/-/DCSupplemental.

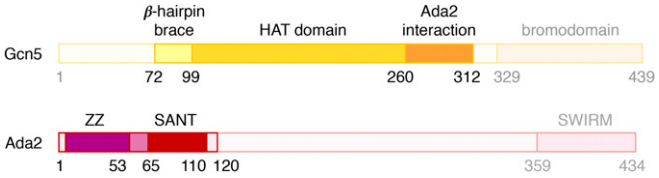

Fig. 1. Structural and functional domains of Gcn5 and Ada2. The Gcn5 residues observed in Ada2/Gcn5 crystal form 1 (residues 72–312) are shown in saturated colors, and the residues outside this region are shown in faded colors. A similar convention is used to highlight the Ada2 residues observed in Ada2/Gcn5 crystal form 1 (residues 1–120).

histone tail-binding module, as it is positioned away from the Gcn5 peptide-binding pocket. Instead, our studies indicate that the Ada2 SANT activates Gcn5's HAT activity by enhancing binding of the acetyl-CoA cosubstrate.

Results

Crystallization and Structure Determination of Ada2/Gcn5 Complexes. We had previously determined through deletion analysis that Gcn5(67-328) was sufficient to form a complex with Ada2(1-120) with robust HAT activity (30). This region of Gcn5 includes N- and C-terminal extensions to the HAT catalytic domain (residues 99–259) and the previously determined Ada2-interacting domain (residues 260–280; Fig. 1). Ada2(1-120) includes the SANT domain known to enhance Gcn5's catalytic activity as well as the ZZ zinc-binding domain.

Crystallization trials of Ada2(1-120)/Gcn5(67-328) produced single 200 × 200 × 200-μm crystals, but these crystals diffracted X-rays only to 8 Å (30). Postcrystallization dehydration beneficial for other macromolecular crystals did not improve the diffraction. Crystals with similar morphology and diffraction properties were also grown by using Ada2(1-120)/Gcn5(67-317) (31), truncated slightly on the Gcn5 C-terminal end. However, efforts to grow crystals with improved diffraction properties by (*i*) manipulating the precise N or C termini of yeast Ada2 and Gcn5, (*ii*) employing other species of Ada2 and Gcn5, (*iii*) engineering surface entropy mutations, or (*iv*) employing fusion proteins with rigid linkers were unsuccessful (30, 31).

Abs, especially mAbs, have been employed as crystallization chaperones to grow crystals of intractable macromolecules such as membrane proteins (32–34). Instead of preparing monoclonal antibodies, we used phage display to screen in vitro for synthetic Abs (sABs), which are functionally and structurally similar to Fabs (35). Biochemical screening against the Ada2(1-120)/Gcn5(67-317) complex produced 17 sABs, 12 of which bound to the Ada2(1-120)/Gcn5(67-317) complex in size-exclusion chromatography binding experiments. Ada2(1-120)/Gcn5(67-317)/sAB complexes corresponding to 9 of the 12 sABs were purified by size exclusion and subjected to crystallization experiments. Three such complexes produced crystals, two of which (referred to as Ada2/Gcn5 crystal forms 1 and 2) diffracted X-rays to 2.7 Å and 2.0 Å, respectively.

We determined the crystal structures of Ada2/Gcn5 crystal forms 1 and 2 by molecular replacement, using as search models the NMR structure of a SANT domain [Protein Data Bank (PDB) ID code 2ELK], the crystal structure of yeast Gcn5 HAT domain (PDB ID code 1YGH) (11), and the crystal structure of an sAB molecule used to crystallize a protein targeting complex (PDB ID code 4XTR) (36). The crystallographic asymmetric unit for the Ada2/Gcn5 crystal form 1 contains one copy each of Ada2, Gcn5, and the sAB (Fig. 2*A*), whereas the asymmetric unit for Ada2/Gcn5 crystal form 2 contains two copies of each (*SI Appendix*, Fig. S1). As expected, the CDRs of the sABs form the antigen (Ada2/Gcn5) binding site (Fig. 2). Interestingly, the two different sABs in crystal forms 1 and 2 interact with similar regions of the Ada2/Gcn5 complex, with the sAB in crystal form 1 making more extensive interactions with Ada2 and Gcn5, whereas the sAB in crystal form 2 contacts Gcn5 predominantly (Fig. 2). The sABs are responsible for the critical crystal contacts for crystal forms 1 and 2 (*SI Appendix*, Fig. S2), highlighting the integral role of the sABs in producing these crystals.

Interactions Between Ada2 and Gcn5. The crystal structures of yeast Ada2/Gcn5 crystal forms 1 and 2 show an elongated three-lobed complex with dimensions 80 × 50 × 40 Å (Fig. 3). The three lobes correspond to the torso, shoulders, and head of the complex. The complex's Gcn5 HAT domain (Gcn5 residues 99–259), which constitutes the torso lobe, is very similar in structure to the yeast Gcn5 HAT domain on its own (rmsd = 0.51 Å for all atoms), with only localized differences in the flexible histone peptide binding loop, the CoA binding loop, and the N-terminal region (*SI Appendix*, Fig. S3*A*). The N- and C-terminal extensions to the Gcn5 HAT domain interact with the Ada2 ZZ and SANT domains predominantly through hydrophobic contacts to form the shoulder and head lobes. The shoulder lobe is composed of an α-helix corresponding to Gcn5 residues 260–280 (immediately C-terminal to the HAT domain) flanked by the Ada2 SANT domain on one side and a β-hairpin from the Gcn5 N-terminal extension to the HAT domain ("β-hairpin brace," residues 72–98) on the other side. This Gcn5 α-helix corresponds to the same region identified as the Ada2 interaction region in biochemical deletion experiments (26). The head lobe is comprised of the Gcn5 extended chain residues 283–312, which cradle the Ada2 ZZ domain (the two zinc atoms in the ZZ domain can be thought of as eyes in the head region; Fig. 3). The extensive and multivalent interaction between Ada2 and Gcn5 provides a structural explanation for why partial deletion of the Ada2 ZZ domain or the SANT domain did not prevent formation of the Ada2/Gcn5 complex or the SAGA complex (27, 28).

Conformational Flexibility Within Ada2/Gcn5 Complex. Although the overall structure of the Ada2/Gcn5 complex is similar in crystal forms 1 and 2, there are notable conformational differences away from the Gcn5 HAT domain in the two crystal forms. The torso lobes (Gcn5 HAT domain) and the shoulder lobes (which contain Ada2 SANT domain) of crystal forms 1 and 2 align very well (rmsd = 0.44 Å for all atoms), but the head lobes (which contain the Ada2 ZZ domain) are rotated by 16° in the two crystal forms (*SI Appendix*, Fig. S4*A*). The head lobes of crystal forms 1 and 2 themselves are very similar (rmsd = 0.47 Å for all atoms), and the differences between crystal forms 1 and 2 are mostly isolated

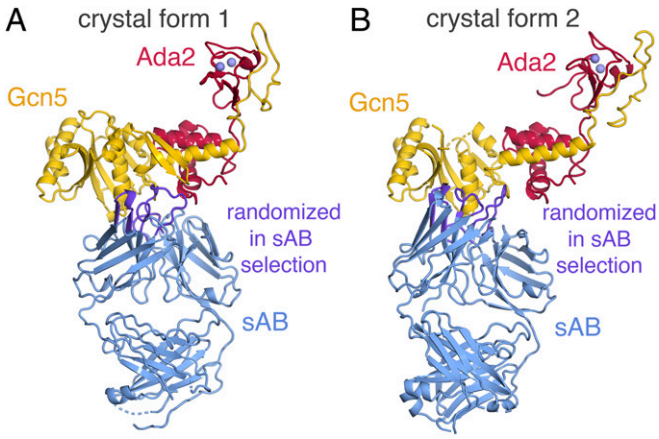

Fig. 2. Ada2/Gcn5 crystal forms 1 and 2 structures. (*A*) Crystal form 1 with Ada2, Gcn5, the sAB, and zinc ions shown in red, yellow, blue, and lavender, respectively. The sAB regions randomized in the selection process are shown in purple. Internal disordered regions of 10 residues or less are shown in dashes. (*B*) Crystal form 2 with the same coloring conventions as for *A*.

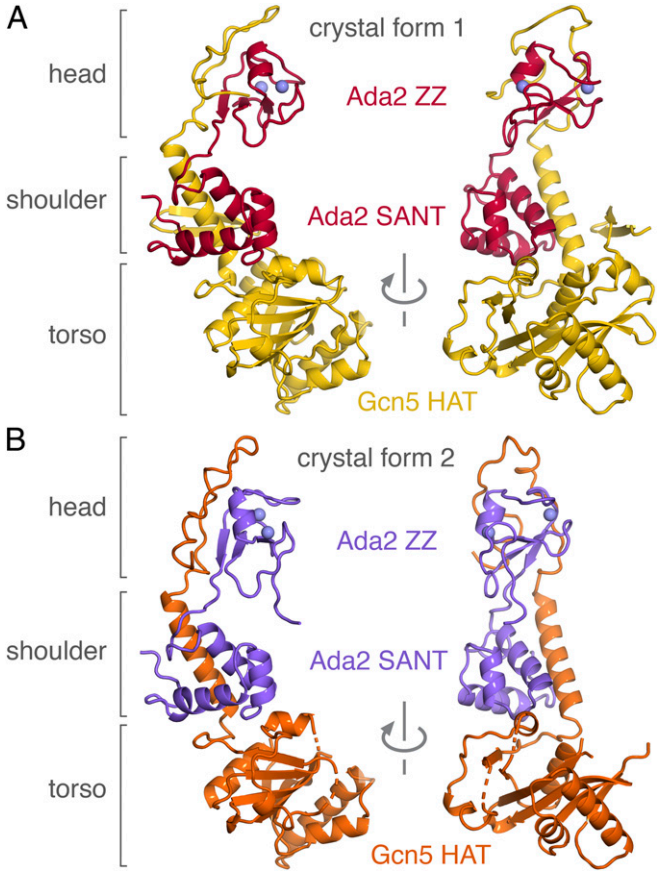

Fig. 3. Comparison of Ada2/Gcn5 crystal forms 1 and 2. (*A*) Crystal form 1 with Gcn5 shown in yellow and Ada2 in red. (*B*) Crystal form 2 with Gcn5 in orange and Ada2 in purple.

to rigid body rotation of the head lobes (*SI Appendix*, Fig. S4*B*). Crystal form 1's head lobe is rotated toward the torso lobe compared with crystal form 2's head lobe. The shoulder lobe is rigidly positioned next to the torso lobe because of the tight packing of the Ada2 SANT domain in the shoulder lobe against the Gcn5 HAT domain that constitutes the torso lobe. In contrast, there are relatively few interactions binding the head lobe to the shoulder domain. These observations suggest that the head lobe of the Ada2/Gcn5 complex is flexibly linked to the shoulder and torso lobes in solution. The different Ada2/Gcn5 complex conformations were stabilized in crystal forms 1 and 2 by the sAB molecules, which mediate the critical crystal contacts. We speculate that this conformational flexibility within the Ada2/Gcn5 complex contributed to the relatively poor internal order of our original Ada2/Gcn5 crystals grown in the absence of the sAB crystallization chaperones.

Mechanism of HAT Activation by Ada2. The Ada2/Gcn5/sAB complex crystals were grown in the absence of substrate histone peptides or CoA. However, given the strong structural similarity between the yeast and *Tetrahymena* Gcn5 HAT domains and the absence of significant conformational changes between the HAT domain in Gcn5 vs. Ada2/Gcn5, we could model by simple superposition the substrate peptide and CoA binding based on the *Tetrahymena* crystal structures containing an 11- or 19-residue H3 peptide and CoA (13, 15) (Fig. 4). The Gcn5 HAT domain binds the histone peptide substrate in a pocket that is positioned away from the Ada2 SANT domain. If the Ada2 SANT domain and the Gcn5 Ada2 interaction helix make up the shoulder of the Ada2/Gcn5 complex, the histone peptide substrate-binding pocket is located in the lower torso of the complex. No direct contacts between the modeled 19-residue H3 peptide and the Ada2 SANT or ZZ domains are possible. [The closest contact between the modeled H3 peptide and the Ada2 SANT domain is 16.8 Å. This and other analysis (detailed later) was made with the use of Ada2/Gcn5 crystal form 1 because of fewer unstructured loops in this crystal form despite the lower resolution, but the structural conclusions are consistent with both crystal forms.] It is therefore difficult to account for Ada2's activation of Gcn5's HAT activity, especially given that we did not observe significant conformational changes within the Gcn5 HAT domain in the Ada2/Gcn5 complex.

Histone acetylation by Gcn5 requires two substrates: the histone peptide and acetyl-CoA. Gcn5 forms a ternary complex with its two substrates before catalysis, with acetyl-CoA binding first, followed by the histone peptide (10). Like the modeled histone peptide, the modeled CoA does not directly contact Ada2 in our structure: the closest contact is between the 3′ phosphate group of CoA and the SANT domain at approximately 6 Å. Although the electron density for the Gcn5 Lys223 side chain is weak (*SI Appendix*, Figs. S5 and S6), this modeled CoA 3′ phosphate group appears to hydrogen-bond with the terminal amino group of Gcn5 Lys223 from the HAT domain and to make additional electrostatic interactions with the guanidinium group of Gcn5 Arg89 from the β-hairpin brace N-terminal extension to the HAT domain (Fig. 4).

The Gcn5 Lys223 side chain that contacts the modeled CoA 3′ phosphate group lies on the same surface that interacts with the Ada2 SANT domain. In fact, the Ada2 SANT domain forms a

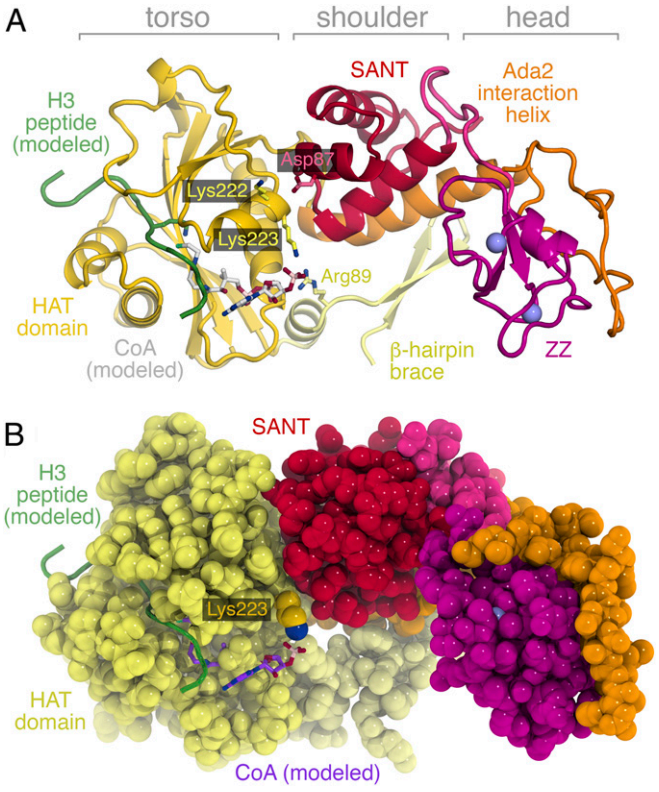

Fig. 4. Ribbon and space-filling representations of the Ada2/Gcn5 complex with modeled H3 peptide substrate (green) and CoA (white or purple) cosubstrate from PDB ID code 1PU9. (*A*) Cartoon representation of the Ada2/Gcn5 complex showing Gcn5 Lys223 and Arg89 side chains interacting with the modeled CoA cosubstrate. The Ada2 SANT and ZZ domains are positioned too far away to directly interact with the H3 peptide substrate or the CoA cosubstrate. Ada2 Asp87 and Gcn5 Lys222 side chains are also shown. (*B*) Space-filling representation of the Ada2/Gcn5 complex highlights the wall created by the Ada2 SANT domain to constrain the Lys223 side chain and promote interaction with the CoA cosubstrate.

wall that constrains the position of the Gcn5 Lys223 side chain (Fig. 4*B*). The main chain oxygen of Leu80 in the Ada2 SANT domain makes very close contact with the Ca atom of Gcn5 Lys223 (3.1 Å), whereas the main chain oxygen of Thr79 is near (4.4 Å) the apparent position of the epsilon carbon of the Lys223 side chain. It is worth noting that only main-chain atoms of Ada2 contact Gcn5 Lys223 and that no amino acid side chain from the Ada2 SANT domain appears to interact with Gcn5 Lys223. These structural observations suggest that Ada2 activates Gcn5's HAT activity because the Ada2 SANT domain constrains the Gcn5 Lys223 side chain to adopt a conformation appropriate for interacting with CoA through the CoA phosphate group.

To test this hypothesis, we prepared point mutations in Gcn5 and Ada2 and examined the HAT activity against an H3 peptide (Table 1). Compared with Gcn5 alone, the Ada2/Gcn5 complex had more than 100-fold higher catalytic efficiency (k_{cat}/K_m) in 10 μM acetyl-CoA, resulting from a 26-fold increase in the catalytic rate constant and a fourfold decrease in the Michaelis constant (*SI Appendix*, Fig. S7). Removing the Gcn5 Lys223 side chain dramatically reduced the catalytic efficiency of the Ada2/Gcn5 complex (~18-fold reduced vs. WT complex) by affecting the k_{cat} and the K_m. In fact, the K_m of the Ada2/Gcn5(K223A) mutation was greater than that of Gcn5 on its own. Mutation of Arg89 had a smaller effect: the k_{cat}/K_m of the Ada2/Gcn5(R89A) complex was only 2.7-fold lower than that of the WT Ada2/Gcn5 complex. Mutating Ada2 D87A had a statistically insignificant effect, consistent with the incidental contact between Ada2 Asp87 and Gcn5 Lys222, compared with the much more extensive interactions between the Ada2 SANT domain and the Gcn5 HAT domain and the Gcn5 Ada2 interaction helix (Fig. 4). Removing both K223 and R89 side chains in the Ada2/Gcn5 complex eliminated the Ada2-mediated enhancement of Gcn5's HAT activity, with a similar k_{cat}/K_m to that of Gcn5 alone. At much higher concentrations of acetyl-CoA [10× higher than the K_d (as detailed later) or 600 μM when the K_d could not be determined], only Ada2/Gcn5 complexes with mutations in K223 or R89 showed significantly increased k_{cat}/K_m, which was attributable mostly to decreases in K_m (Table 1 and *SI Appendix*, Fig. S8). The partial compensation of increased acetyl-CoA concentrations for the removal of K223 and R89 is consistent with the proposed roles of these side chains in recruiting acetyl-CoA. We also find that the HAT activity of the Ada2/Gcn5 complex was not altered significantly when assayed in the presence of the sAB used to crystallize the Ada2/Gcn5 complex in crystal form 1, indicating that the antibody does not affect the catalytic activity of Ada2/Gcn5. This agrees with our structural finding that the sAB binds Ada2 and Gcn5 away from the H3 peptide and acetyl-CoA binding sites in Gcn5.

We further assessed the role of Gcn5(K223A) by examining its effect in the Gcn5 protein or in the Ada2/Gcn5 complex. We find that Gcn5(K223A) has a smaller effect, particularly on the K_m for histone H3 in saturating or near-saturating concentrations of acetyl-CoA. Compared with Gcn5 alone, the K_m of histone H3 for Ada2/Gcn5 is increased 7.2 fold, whereas the equivalent K_m for Ada2/Gcn5(K223A) is increased only 2.8 fold (Table 1). This is consistent with a Gcn5 K223-dependent role for Ada2 in Ada2/Gcn5's HAT activity.

The HAT activity results suggest that the Gcn5 Lys223 side chain plays a major role by interacting with acetyl-CoA. To investigate this directly, we measured acetyl-CoA binding by isothermal calorimetry (Table 1 and *SI Appendix*, Fig. S9). We find that Gcn5 binds acetyl-CoA with a K_d of 7.8 μM, similar to the 8.5-μM K_d measured by equilibrium dialysis for the yeast Gcn5 catalytic domain (37). The Ada2/Gcn5 complex binds acetyl-CoA with a K_d of 2.3 μM, or 3.4-fold more tightly. Strikingly, the Ada2/Gcn5(K223A) and the Ada2/Gcn5(R89A,K223A) complexes fail to bind acetyl-CoA, whereas the Ada2/Gcn5(R89A) complex binds 15.7× less tightly than the WT Ada2/Gcn5 complex. The Ada2 (D87A)/Gcn5 complex binds acetyl-CoA with a similar affinity as the WT complex, consistent with the insignificant effect of this mutation on the HAT activity. These acetyl-CoA binding studies indicate that yeast Gcn5 Lys223 plays a critical role in binding acetyl-CoA and that Ada2 enhances acetyl-CoA binding by Gcn5 even though Ada2 does not appear to interact directly with acetyl-CoA.

We also used calorimetry to investigate whether Ada2 affects binding of Gcn5's binding of its H3 peptide substrate. We find that Gcn5 and Ada2/Gcn5 bind the H3 peptide with similar affinities, suggesting that Ada2 does not activate Gcn5 by promoting histone peptide binding (*SI Appendix*, Fig. S10 and Table S2). Similar results were obtained in the presence of CoA.

Discussion

The crystal structures of the Ada2/Gcn5 complex provide insights into how the Gcn5 catalytic HAT domain, together with N- and C-terminal extensions, binds to the Ada2 ZZ and SANT domains. Extensive contacts mediate the interactions between the two proteins, suggesting that they cooperatively assemble to form their stable structure, as it is likely that many of the structural elements in the complex would be unfolded on their own. For example, the β-hairpin brace and Ada2 interaction helix of Gcn5 are stabilized by their intramolecular interactions and the intermolecular interaction of Gcn5's Ada2 interaction helix with the Ada2 SANT domain. Gcn5 residues 283–312 form an extended chain platform to bind to the Ada2 ZZ domain, and are likely disordered in the absence of Ada2.

The structures suggest a mechanism for how Ada2 increases Gcn5's HAT activity. Several studies have documented that the Ada2 SANT domain is required for the activation of Gcn5's HAT activity in the Ada2/Gcn5 subcomplex or the full SAGA complex (27–29). A kinetic analysis of the Ada2/Gcn5 complex showed that deleting the Ada2 SANT domain reduced H3 peptide substrate binding and catalysis, but apparently not acetyl-CoA binding (28).

Table 1. HAT activity and AcCoA isothermal calorimetry binding data for Gcn5(67-317) and Ada2(1-120)/Gcn5(67-317) variants

Samples			Catalysis in 10 μM AcCoA				Catalysis at higher AcCoA concentrations				AcCoA binding
Ada2	Gcn5	sAB	[AcCoA], μM	k_{cat}, s^{-1}	K_m, μM	k_{cat}/K_M, $M^{-1}\cdot s^{-1}$	[AcCoA], μM	k_{cat}, s^{-1}	K_m, μM	k_{cat}/K_M, $M^{-1}\cdot s^{-1}$	AcCoA K_d, μM
–	+	–	10	0.048 ± 0.003	749 ± 112	65	100	0.102 ± 0.014	1,348 ± 400	75	7.8 ± 3
–	K223A	–	—	—	—	—	600	0.047 ± 0.003	802 ± 123	59	ND
+	+	–	10	1.28 ± 0.12	189 ± 62	6,790	24	1.27 ± 0.076	187 ± 38	6,780	2.3 ± 0.2
+	K223A	–	10	0.414 ± 0.029	1110 ± 175	372	600	0.430 ± 0.048	291 ± 103	1,480	NA
+	R89A	–	10	0.917 ± 0.085	364 ± 97	2,520	400	0.724 ± 0.078	187 ± 78	3,870	36.2 ± 5.5
+	R89A,K223A	–	10	0.096 ± 0.006	1930 ± 212	50	600	0.209 ± 0.023	771 ± 182	271	NA
D87A	+	–	10	1.06 ± 0.11	191 ± 76	5,570	30	1.15 ± 0.14	213 ± 97	5,420	2.7 ± 0.6
+	+	+	10	1.34 ± 0.096	156 ± 41	8,570	30	1.51 ± 0.16	156 ± 59	9,670	ND

Columns 4–7 show catalysis results in 10 μM AcCoA, columns 8–11 show catalysis results in near-saturating conditions of AcCoA, and column 12 shows AcCoA binding data. conc, concentration; NA, not applicable (because no binding detected); ND, not determined.

This finding led to the hypothesis that the Ada2 SANT domain functions as a histone tail-binding/presentation module. Our studies suggest a different mechanism. We find that the Ada2 SANT is far removed from the Gcn5 peptide binding pocket and also too far to make direct contact with CoA. However, it does contact Gcn5 Lys223, which itself appears to directly interact with CoA through the CoA 3′ phosphate group. The SANT domain creates a physical barrier that constrains the conformational flexibility of the Lys223 side chain and could help direct the side chain for productive interaction with the 3′ phosphate group of acetyl-CoA. As binding of acetyl-CoA by Gcn5 is the necessary first step in the catalytic mechanism before binding a histone peptide (10), enhancing acetyl-CoA binding will increase Gcn5's HAT activity. The Ada2 SANT domain thus functions to complete the CoA binding pocket on Gcn5. The Gcn5 N-terminal extension of an α-helix plus the β-hairpin brace also contributes toward this acetyl-CoA binding pocket, with Arg89 residue apparently interacting with the same 3′ phosphate group of acetyl-CoA (Fig. 4). In hindsight, it is not surprising that Ada2 can influence Gcn5's HAT activity by modulating interactions with acetyl-CoA, as acetyl-CoA is a cosubstrate in the histone acetylation reaction.

Our results define what has been a nebulous role of Lys223 in Gcn5's HAT activity. Partially pure recombinant Gcn5(K223A) displayed reduced HAT activity in vitro and a more modest effect of the mutant on transcriptional activity in yeast (38). It should be noted that the steady-state transcriptional assay used in this study masks SAGA complex's now recognized role in generating newly synthesized mRNA transcripts (39). A triple Gcn5(F221A,K222A, K223A) mutant was found to be strongly defective for growth and in vivo transcriptional activity (40), but a specific effect of K223A cannot be determined from this result because subsequent crystal structures show that F221 is part of the hydrophobic core of the Gcn5 HAT domain. Another study found that Gcn5 (K223A, T227A,K228A,E229A) and Gcn5(K223A,T227A,K242A) surface mutations severely affected HAT activity in vitro and displayed partial growth defects (27). In crystal structures of *Tetrahymena* Gcn5 HAT domain bound to H3 peptide CoA, the equivalent lysine points its side chain away from the CoA phosphate group (13). Interestingly, the only structure of the yeast Gcn5 HAT domain crystallized without CoA or substrate peptide shows Lys223 in a similar conformation to what we observed in Ada2/Gcn5 (11).

The critical role of yeast Gcn5 Lys223 in binding acetyl-CoA is likely to be preserved in Gcn5 orthologs, as this lysine residue is strictly conserved from yeast to plants to mammals (*SI Appendix*, Fig. S11). In contrast, the minor role of yeast Gcn5 Arg89 in binding acetyl-CoA among Gcn5 orthologs is more difficult to predict. Although the sequence alignment in *SI Appendix*, Fig. S11 suggests that Gcn5 Arg89 is not conserved among species, an arginine amino acid two residues before this position in many species could possibly function to bind acetyl-CoA.

The Ada2/Gcn5 complexes in the two different crystal forms highlights a general conformational flexibility, in particular that of the head lobe containing the Ada2 ZZ domain, which is tethered to the Ada2 SANT domain-containing shoulder lobe via relatively mobile connections. The functional significance of this conformational flexibility within the Ada2/Gcn5 complex is uncertain. This is because Ada2/Gcn5 is only part of the Ada3/Ada2/Gcn5 HAT module, itself part of the full SAGA complex. It is possible that the conformational flexibility between the head and shoulder lobes is an artifact of the isolated and truncated Ada2/Gcn5 subcomplex investigated here and that binding of Ada3 or remaining regions of Ada2 or Gcn5 will fix the orientation between the head and shoulder domains. It is also possible that the conformational flexibility between the head and shoulder domains could play a functional role within the SAGA complex for nucleosomal acetylation.

Our determination of the crystal structure of the Ada2/Gcn5 complex relied on the use of synthetic antibodies as crystallization chaperones, an approach that is gaining increasing attention because of its demonstrated successes in crystallizing recalcitrant protein systems. In this regard, an important recent advance has been the use of phage display to generate sABs. It has proven to produce a much larger variety of binders, much faster and cheaper than traditional monoclonal approaches. Importantly, the methodology allows for selection conditions that can be designed to produce sABs with desired characteristics; for instance, sABs that bind to a particular surface epitope or conformational state of the target protein. Notably, the Ada2/Gcn5 biopanning conditions were highly biased toward selecting sABs that recognized the assembled complex, not the individual protein components. This stabilizes the macromolecular assemblage during crystallization into the form that is most biologically relevant. We speculate that our crystals of the Ada2/Gcn5 grown in the absence of sABs were limited to 8-Å diffraction because of the flexible link between the head and shoulder lobes observed in the two crystal forms. Examination of the crystal packing in Ada2/Gcn5 crystal forms 1 and 2 shows how the respective synthetic antibodies build the crystal through antibody/antibody interactions (*SI Appendix*, Fig. S2), and the resulting packing stabilizes the otherwise flexible Ada2/Gcn5 complex.

In summary, our structural and biochemical studies reveal mechanistic insights for how an accessory or partner protein can influence the enzymatic activity of a HAT: by affecting binding of the acetyl-CoA substrate instead of the histone substrate. We suspect that similar mechanisms will be employed by other histone modification enzymes.

Materials and Methods

Protein Expression and Purification. Ada2 residues 1–120 [N-terminally tagged with hexahistidine and maltose binding protein (MBP)] and Gcn5 residues 67–317 were coexpressed by using the pST44 polycistronic expression vector (41, 42). Site-directed mutations were introduced by using QuikChange-based procedures (43) employing Q5 DNA polymerase (New England Biolabs). Protein expression in BL21(DE3)pLysS host strains were induced with 0.2 mM IPTG at 18 °C.

Ada2/Gcn5 complexes were purified from cell lysates by cobalt metal affinity chromatography (Talon resin; Clontech), followed by TEV protease cleavage to remove the HISMBP tag and SourceS cation-exchange chromatography (GE Healthcare). As Gcn5(67-317) proved difficult to purify on its own, we first purified the Ada2/Gcn5 complex and then used mildly denaturing conditions (3 M urea) to dissociate the complex and to isolate Gcn5(67-317) by SourceS chromatography. The SourceS Gcn5(67-317) pool was then further purified by Superdex 200 Increase 10/300 size-exclusion chromatography (GE Healthcare).

sAB Selection, Characterization, Expression, and Purification. The generation and screening of complex-specific sABs has been described previously (44). Two N-terminally Avi-His-TEV-tag modified Ada2/Gcn5 complexes were prepared whereby the affinity tag was placed on Ada2 or Gcn5. Both proteins were expressed, biotinylated in vivo, purified, and tested for biotinylation efficiency. Three rounds of phage display selection were performed by using 100 nM (round 1), 50 nM (round 2), and 10 nM (round 3) biotinylated protein targets and each time eluted with TEV protease (Thermo). After successful selection, the specificity of candidate sABs was assayed against both Avi-tagged complexes by using a single point competitive ELISA (44). Clones that exhibited strong and specific binding to both antigens were sequenced. We obtained more than 30 sequence-unique sABs, and 17 were nominated for further biochemical characterization. All sABs were characterized for their ability to stabilize Ada2/Gcn5 complex by gel filtration in 20 mM Hepes, 100 mM NaCl, 10 mM β-mercaptoethanol, pH 7.5, buffer on a Superdex 200 Increase 10/300 column (GE Healthcare). Only sABs that formed the most homogenous complex were systematically tested in crystallization trials.

sAB clones were expressed and purified by using dual-column chromatography using Protein A affinity (HiTrap MabSelect SuRe, 5 mL), immediately followed by ion exchange (Resource S, 1 mL) as previously described (44). Samples were dialyzed against 20 mM Hepes, 100 mM NaCl, pH 7.5, concentrated to more than 10 mg/mL and frozen in 100-μL aliquots.

yGcn5/yAda2/sAB Crystallization and Structure Determination. Gcn5/Ada2 complex was incubated with 1.2 molar excess of sAB and purified by Superdex 200 Increase 10/300 size-exclusion chromatography in 20 mM Hepes, pH 7.5, 100 mM NaCl, 10 mm 2-mercaptoethanol. Pooled fractions were concentrated to approximately 10 mg/mL and used for microbatch under oil crystallization trials (45). Crystal form 1 containing 65H10_1 synthetic antibodies

was grown in 10 mM Tris·Cl, pH 8.5, 200 mM Li_2SO_4, and 25% wt/vol PEG3350, whereas crystal form 2 containing 63E9_24 synthetic antibodies was grown in 100 mM succinic acid, pH 7.0, and 15% wt/vol PEG3350.

Before flash-cooling in liquid nitrogen, crystal form 1 crystals were soaked in the crystallization solution supplemented with 20% vol/vol glycerol in 5% glycerol steps, whereas crystal form 2 crystals were soaked in their crystallization solution supplemented with 25% wt/vol PEG3350 in 5% PEG3350 steps.

X-ray diffraction data were collected at Advanced Photon Source NE-CAT beamline 24-ID-C (0.9792 Å; 100K). The diffraction data were processed by using XDS (46) and SCALA (47) software packages. Molecular replacement using PHASER (48) employed rigid body search models from the HAT domain of yGcn5 (PDB ID code 1YGH), a SANT domain homolog (PDB ID code 2ELK), and the sAB from the Get3–sAB complex (PDB ID code 4XTR). Structure refinement was performed with the programs REFMAC (49) and PHENIX (50) together with manual model building in COOT (51). Crystallographic data statistics are summarized in *SI Appendix*, Table S1. All molecular graphics were prepared with PyMOL (52).

HAT Assay. HAT activity was measured by using a pyruvate dehydrogenase enzyme-coupled assay (53) with substrate H3 peptide residues 1–20 (ARTKQTARKSTGGKAPRKQL). Each reaction contained 1× TBA (50 mM Tris, 50 mM Bis·Tris, 100 mM sodium acetate, pH 7.5), 5 mM $MgCl_2$, 1 mM DTT, 0.2 mM thiamine pyrophosphate, 0.2 mM NAD+, 2.5 mM pyruvate, 0.04 U pyruvate dehydrogenase, and 0.25 μM Ada2/Gcn5 or Gcn5 enzyme. Specified concentrations of acetyl-CoA were included, with the highest concentration of 600 μM chosen because we observed inhibition at greater than this concentration. The reaction mixture was incubated at room temperature for 5 min before the reaction was initiated by adding the enzyme. The reaction was monitored in real time at 340 nm in a Varian Cary 50 Bio spectrophotometer.

Isothermal Titration Calorimetry. Calorimetric experiments were conducted at 25 °C with a MicroCal auto-iTC200 instrument (Malvern). The protein samples were dialyzed against the buffer containing 20 mM Hepes (pH 7.5), 100 mM NaCl, and 2 mM β-mercaptoethanol. The exothermic heat of the reaction for acetyl-CoA binding was measured by 25 sequential 1.5-μL injections of 100 μM acetyl-CoA into 200 μL of 10 μM Gcn5 or Ada2/Gcn5 complex, spaced at intervals of 180 s. To further saturate Ada2/Gcn5(R89A), 200 μM acetyl-CoA was titrated into 10 μM of this mutant complex. Histone H3 binding was measured with similar injections of 800 μM H3(1-20) peptide into 200 μL of 80 μM Gcn5 or Ada2/Gcn5 complex with or without 80 μM CoA present. The data were analyzed by using the Origin 7 software package (Microcal).

ACKNOWLEDGMENTS. We are very grateful to the staff of APS NE-CAT beamlines 24-ID-C and 24-ID-E for their help during synchrotron data collection, J. Fecko and N. Yennawar (Penn State Huck Institute X-ray core facility) for assistance with isothermal calorimetry and crystallographic refinement, and members of the laboratory of S.T., Phil Bevilacqua, and the Penn State Center for Eukaryotic Gene Regulation for discussions. This work was supported by National Institutes of Health National Institute of General Medical Sciences Grants R01GM088236 (to S.T.), R01GM111651 (to S.T.), U01GM094588 (to A.A.K.), R01GM072688 (to A.A.K.), and U54HG006436 (to A.A.K.).

1. Verdin E, Ott M (2015) 50 years of protein acetylation: From gene regulation to epigenetics, metabolism and beyond. *Nat Rev Mol Cell Biol* 16:258–264.
2. Suganuma T, Workman JL (2011) Signals and combinatorial functions of histone modifications. *Annu Rev Biochem* 80:473–499.
3. Bannister AJ, Kouzarides T (2011) Regulation of chromatin by histone modifications. *Cell Res* 21:381–395.
4. Benton CB, Fiskus W, Bhalla KN (2017) Targeting histone acetylation: Readers and writers in leukemia and cancer. *Cancer J* 23:286–291.
5. Marmorstein R, Zhou M-M (2014) Writers and readers of histone acetylation: Structure, mechanism, and inhibition. *Cold Spring Harb Perspect Biol* 6:a018762.
6. Choi JK, Howe LJ (2009) Histone acetylation: Truth of consequences? *Biochem Cell Biol* 87:139–150.
7. Galvani A, Thiriet C (2015) Nucleosome dancing at the tempo of histone tail acetylation. *Genes (Basel)* 6:607–621.
8. Yuan H, Marmorstein R (2013) Histone acetyltransferases: Rising ancient counterparts to protein kinases. *Biopolymers* 99:98–111.
9. Tanner KG, et al. (1999) Catalytic mechanism and function of invariant glutamic acid 173 from the histone acetyltransferase GCN5 transcriptional coactivator. *J BiolChem* 274:18157–18160.
10. Tanner KG, Langer MR, Kim Y, Denu JM (2000) Kinetic mechanism of the histone acetyltransferase GCN5 from yeast. *J Biol Chem* 275:22048–22055.
11. Trievel RC, et al. (1999) Crystal structure and mechanism of histone acetylation of the yeast GCN5 transcriptional coactivator. *Proc Natl Acad Sci USA* 96:8931–8936.
12. Lin Y, Fletcher CM, Zhou J, Allis CD, Wagner G (1999) Solution structure of the catalytic domain of GCN5 histone acetyltransferase bound to coenzyme A. *Nature* 400:86–89.
13. Rojas JR, et al. (1999) Structure of Tetrahymena GCN5 bound to coenzyme A and a histone H3 peptide. *Nature* 401:93–98.
14. Schuetz A, et al. (2007) Crystal structure of a binary complex between human GCN5 histone acetyltransferase domain and acetyl coenzyme A. *Proteins* 68:403–407.
15. Clements A, et al. (2003) Structural basis for histone and phosphohistone binding by the GCN5 histone acetyltransferase. *Mol Cell* 12:461–473.
16. Clements A, et al. (1999) Crystal structure of the histone acetyltransferase domain of the human PCAF transcriptional regulator bound to coenzyme A. *EMBO J* 18:3521–3532.
17. Wang L, Dent SYR (2014) Functions of SAGA in development and disease. *Epigenomics* 6:329–339.
18. Samara NL, Wolberger C (2011) A new chapter in the transcription SAGA. *Curr Opin Struct Biol* 21:767–774.
19. Baker SP, Grant PA (2007) The SAGA continues: Expanding the cellular role of a transcriptional co-activator complex. *Oncogene* 26:5329–5340.
20. Spedale G, Timmers HTM, Pijnappel WWMP (2012) ATAC-king the complexity of SAGA during evolution. *Genes Dev* 26:527–541.
21. Koutelou E, Hirsch CL, Dent SYR (2010) Multiple faces of the SAGA complex. *Curr Opin Cell Biol* 22:374–382.
22. Grant PA, et al. (1997) Yeast Gcn5 functions in two multisubunit complexes to acetylate nucleosomal histones: Characterization of an Ada complex and the SAGA (Spt/Ada) complex. *Genes Dev* 11:1640–1650.
23. Candau R, Berger SL (1996) Structural and functional analysis of yeast putative adaptors. Evidence for an adaptor complex in vivo. *J Biol Chem* 271:5237–5245.
24. Balasubramanian R, Pray-Grant MG, Selleck W, Grant PA, Tan S (2002) Role of the Ada2 and Ada3 transcriptional coactivators in histone acetylation. *J Biol Chem* 277:7989–7995.
25. Candau R, et al. (1996) Identification of human proteins functionally conserved with the yeast putative adaptors ADA2 and GCN5. *Mol Cell Biol* 16:593–602.
26. Candau R, Zhou JX, Allis CD, Berger SL (1997) Histone acetyltransferase activity and interaction with ADA2 are critical for GCN5 function in vivo. *EMBO J* 16:555–565.
27. Sterner DE, Wang X, Bloom MH, Simon GM, Berger SL (2002) The SANT domain of Ada2 is required for normal acetylation of histones by the yeast SAGA complex. *J Biol Chem* 277:8178–8186.
28. Boyer LA, et al. (2002) Essential role for the SANT domain in the functioning of multiple chromatin remodeling enzymes. *Mol Cell* 10:935–942.
29. Barbaric S, Reinke H, Hörz W (2003) Multiple mechanistically distinct functions of SAGA at the PHO5 promoter. *Mol Cell Biol* 23:3468–3476.
30. Kramer RM (2002) Characterization and crystallization of the yADA2-yGCN5 complex. MS thesis (The Pennsylvania State University, University Park, PA).
31. Barrios AF (2005) Characterization and crystallization of HAT subcomplexes. MS thesis (The Pennsylvania State University, University Park, PA).
32. Griffin L, Lawson A (2011) Antibody fragments as tools in crystallography. *Clin Exp Immunol* 165:285–291.
33. Lieberman RL, Culver JA, Entzminger KC, Pai JC, Maynard JA (2011) Crystallization chaperone strategies for membrane proteins. *Methods* 55:293–302.
34. Bukowska MA, Grütter MG (2013) New concepts and aids to facilitate crystallization. *Curr Opin Struct Biol* 23:409–416.
35. Paduch M, et al. (2013) Generating conformation-specific synthetic antibodies to trap proteins in selected functional states. *Methods* 60:3–14.
36. Mateja A, et al. (2015) Protein targeting. Structure of the Get3 targeting factor in complex with its membrane protein cargo. *Science* 347:1152–1155.
37. Langer MR, Fry CJ, Peterson CL, Denu JM (2002) Modulating acetyl-CoA binding in the GCN5 family of histone acetyltransferases. *J Biol Chem* 277:27337–27344.
38. Kuo MH, Zhou J, Jambeck P, Churchill ME, Allis CD (1998) Histone acetyltransferase activity of yeast Gcn5p is required for the activation of target genes in vivo. *Genes Dev* 12:627–639.
39. Baptista T, et al. (2017) SAGA is a general cofactor for RNA polymerase II transcription. *Mol Cell* 68:130–143.e5.
40. Wang L, Liu L, Berger SL (1998) Critical residues for histone acetylation by Gcn5, functioning in Ada and SAGA complexes, are also required for transcriptional function in vivo. *Genes Dev* 12:640–653.
41. Tan S (2001) A modular polycistronic expression system for overexpressing protein complexes in Escherichia coli. *Protein Expr Purif* 21:224–234.
42. Tan S, Kern RC, Selleck W (2005) The pST44 polycistronic expression system for producing protein complexes in Escherichia coli. *Protein Expr Purif* 40:385–395.
43. Xia Y, Chu W, Qi Q, Xun L (2015) New insights into the QuikChange™ process guide the use of Phusion DNA polymerase for site-directed mutagenesis. *Nucleic Acids Res* 43:e12.
44. Paduch M, Kossiakoff AA (2017) Generating conformation and complex-specific synthetic antibodies. *Methods Mol Biol* 1575:93–119.
45. D'Arcy A, Sweeney AM, Haber A (2004) Practical aspects of using the microbatch method in screening conditions for protein crystallization. *Methods* 34:323–328.
46. Kabsch W (2010) Integration, scaling, space-group assignment and post-refinement. *Acta Crystallogr D Biol Crystallogr* 66:133–144.
47. Evans P (2006) Scaling and assessment of data quality. *Acta Crystallogr D Biol Crystallogr* 62:72–82.
48. McCoy AJ, et al. (2007) Phaser crystallographic software. *J Appl Cryst* 40:658–674.
49. Murshudov GN, Vagin AA, Dodson EJ (1997) Refinement of macromolecular structures by the maximum-likelihood method. *Acta Crystallogr D Biol Crystallogr* 53:240–255.
50. Adams PD, et al. (2010) PHENIX: A comprehensive Python-based system for macromolecular structure solution. *Acta Crystallogr D Biol Crystallogr* 66:213–221.
51. Emsley P, Cowtan K (2004) Coot: Model-building tools for molecular graphics. *Acta Crystallogr D Biol Crystallogr* 60:2126–2132.
52. Schrödinger, LLC (2015) The PyMOL Molecular Graphics System, Version 1.8.
53. Kim Y, Tanner KG, Denu JM (2000) A continuous, nonradioactive assay for histone acetyltransferases. *Anal Biochem* 280:308–314.

PNAS
www.pnas.org

Supplementary Information for

Structural basis for activation of SAGA histone acetyltransferase Gcn5 by partner subunit Ada2

Jian Sun, Marcin Paduch, Sang-Ah Kim, Ryan M. Kramer, Adam F. Barrios, Vincent Lu, Judy Luke, Svitlana Usatyuk, Anthony A. Kossiakoff and Song Tan

Song Tan
Email: sxt30@psu.edu

This PDF file includes:

Figs. S1 to S11
Tables S1 to S2

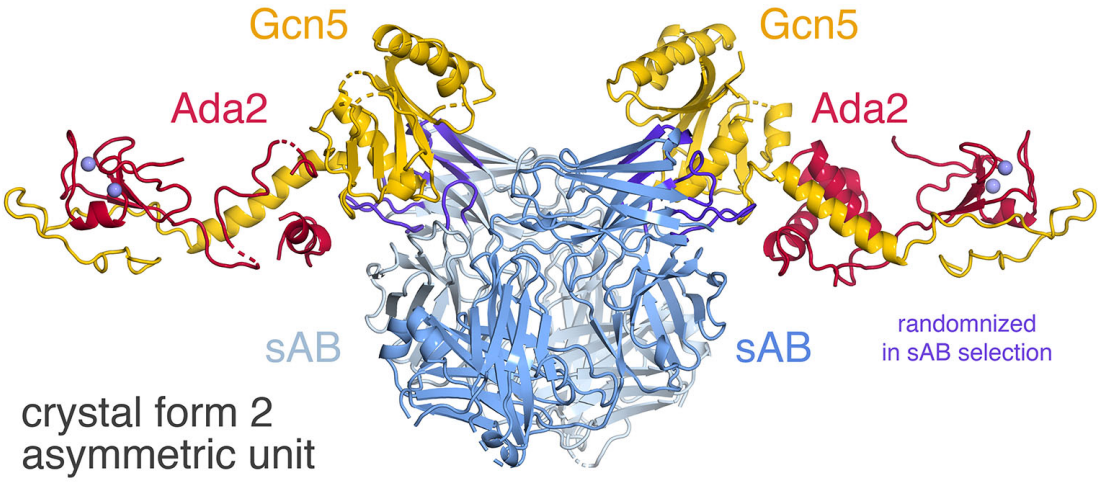

Fig. S1. Asymmetric unit of Ada2/Gcn5 crystal form 2. Unlike Ada2/Gcn5 crystal form 1 which contains one protein complex in the crystallographic asymmetric unit, crystal form 2 contains two Ada2/Gcn5/sAB complexes in the asymmetric unit. Ada2, Gcn5 and the synthetic antibody (sAB) are shown in red, yellow and blue/light blue respectively, while the zinc ions in the Ada2 ZZ domains are shown as lavender spheres. The sAB regions randomized in the selection process are shown in purple.

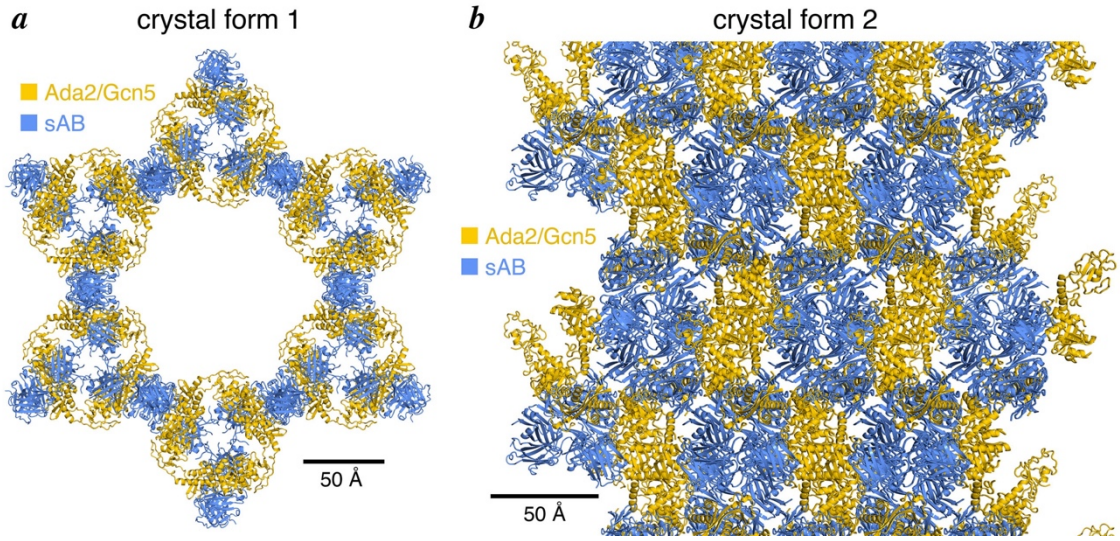

Fig. S2. Crystal packing in Ada2/Gcn5 crystal forms 1 and 2. (a) The Ada2/Gcn5/sAB complexes in crystal form 1 (space group $P3_221$, 2.7 Å resolution) pack to create six-pointed stars with a 125 Å solvent channel through the center. The synthetic antibody (sAB, shown in blue) mediate critical crystal contacts between the Ada2/Gcn5 complex (shown in yellow). (b) Denser packing is apparent for Ada2/Gcn5/sAB complexes in crystal form 2 (space group $P2_12_12_1$, 1.98 Å), but more unstructured loops facing solvent channels result in more missing residues in the structure (including the entire β-hairpin brace). Same colors as for (a).

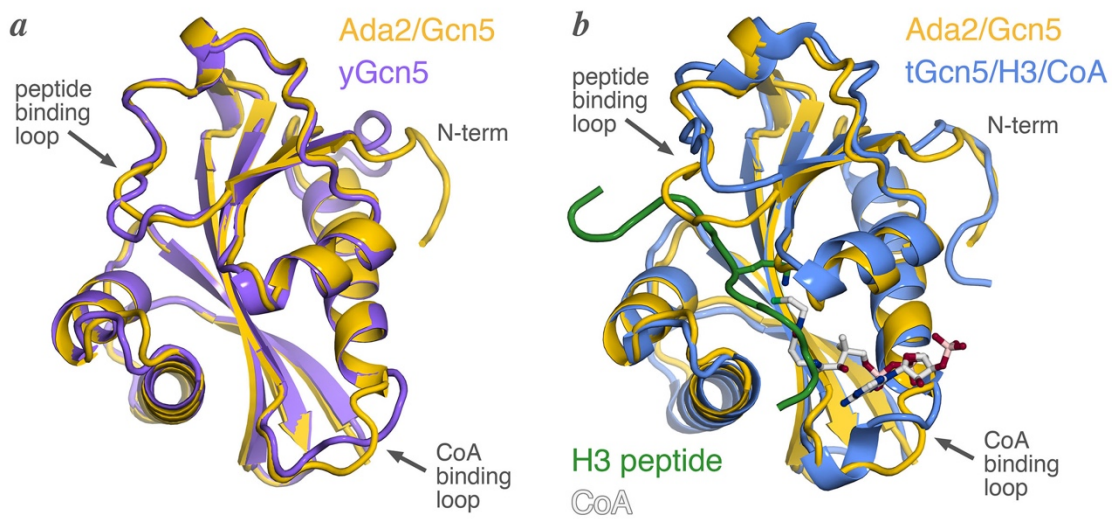

Fig. S3. Comparison of Gcn5 HAT domain structures. (a) Superposition of HAT domain from yeast Ada2/Gcn5 complex (yellow) or yeast Gcn5 (purple, PDB:1YGH) on its own. Neither crystal structure contained substrate peptide or CoA cosubstrate. The HAT domain in the two structures are essentially identical except in the flexible peptide binding loop (between Gcn5 α6 and β9 in the Ada2/Gcn5 complex, equivalent to Gcn5 α5 and β6 in Gcn5 HAT domain only structures), the CoA binding loop and the N-terminal region. (b) Superposition of HAT domain from yeast Ada2/Gcn5 complex (yellow) or *Tetrahymena* Gcn5 (blue) with H3 peptide (green) and CoA (carbons in grey, nitrogen in blue, oxygen in red, phosphate in pink), PDB:1PU9. The flexible Gcn5 peptide binding loop adopts a conformation in the Ada2/Gcn5 complex similar to the conformation observed in the yeast and human Gcn5 HAT domain structures. In these structures crystallized without H3 peptide, the flexible peptide binding loop partly occupies the H3 peptide binding site found in the Tetrahymena Gcn5/H3 peptide structures. As such, the flexible peptide binding loop in the yeast Gcn5, yeast Ada2/Gcn5 and human Gcn5 structures presumably must move for the H3 peptide to bind. However in all crystal structures of the Tetrahymena Gcn5 HAT domain, this flexible peptide binding loop adopts the conformation shown here (blue) whether or not the H3 peptide is present.

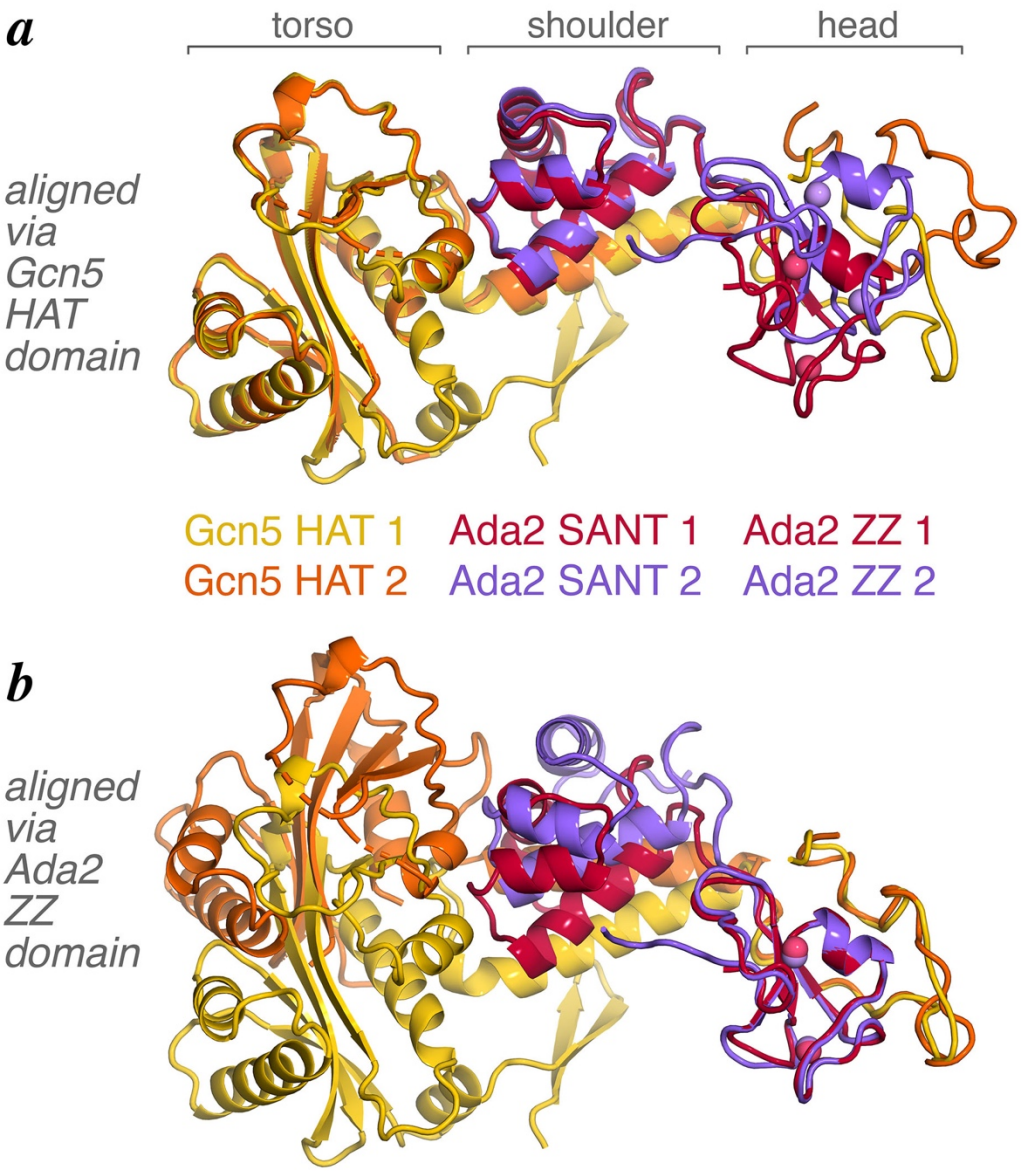

Fig. S4. Conformational differences between Ada2/Gcn5 crystal forms 1 and 2 due to flexing of the head lobe from the torso and shoulder lobes. In crystal from 1, Gcn5 is colored yellow and Ada2 is colored red, whereas in crystal form 2, Gcn5 is colored orange, and Ada2 is colored purple. (a) When aligned via the Gcn5 HAT domain, the torso and shoulder regions of the two crystal forms containing the Ada2 SANT domain and the Gcn5 Ada2 interaction helix superimpose well, but the head region containing the Ada2 ZZ domain and the remainder of the Gcn5 Ada2 interaction region are rotated in the two crystal forms. (b) When aligned via the Ada2 ZZ domain, the ZZ domains in crystal forms 1 and 2 are very similar with some local differences.

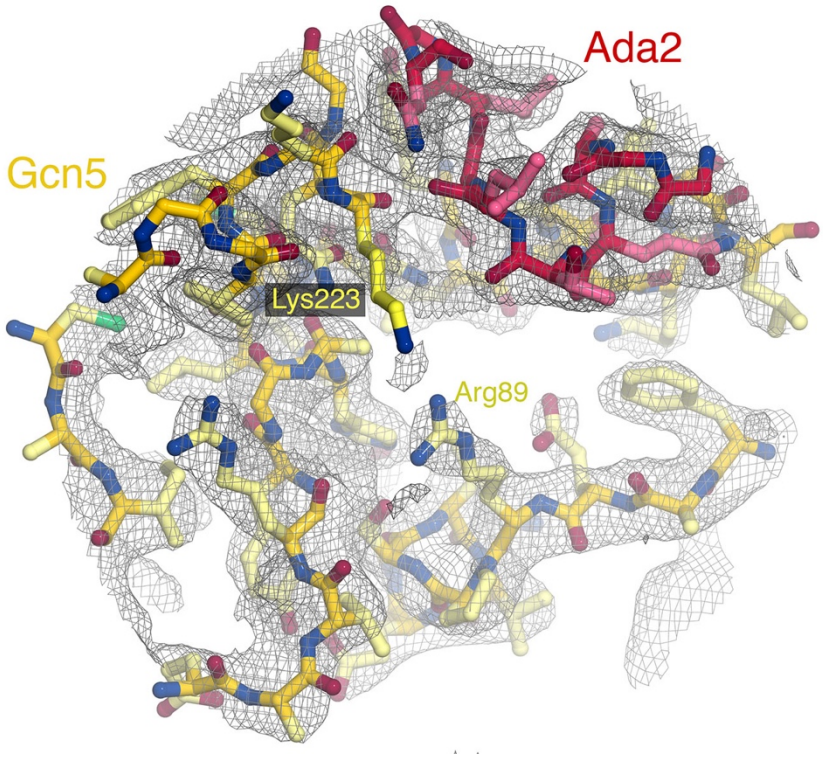

Fig. S5. Electron density of interface between Ada2 and Gcn5 around Gcn5 Lys223. Same orientation as for Fig. 4a and 4b. $2F_o$-F_c map is contoured at 1σ. Main chain and side chain carbon atoms of Gcn5 are shown in dark yellow and light yellow respectively, while main chain and side chain carbon atoms of Ada2 are shown in red and pink respectively.

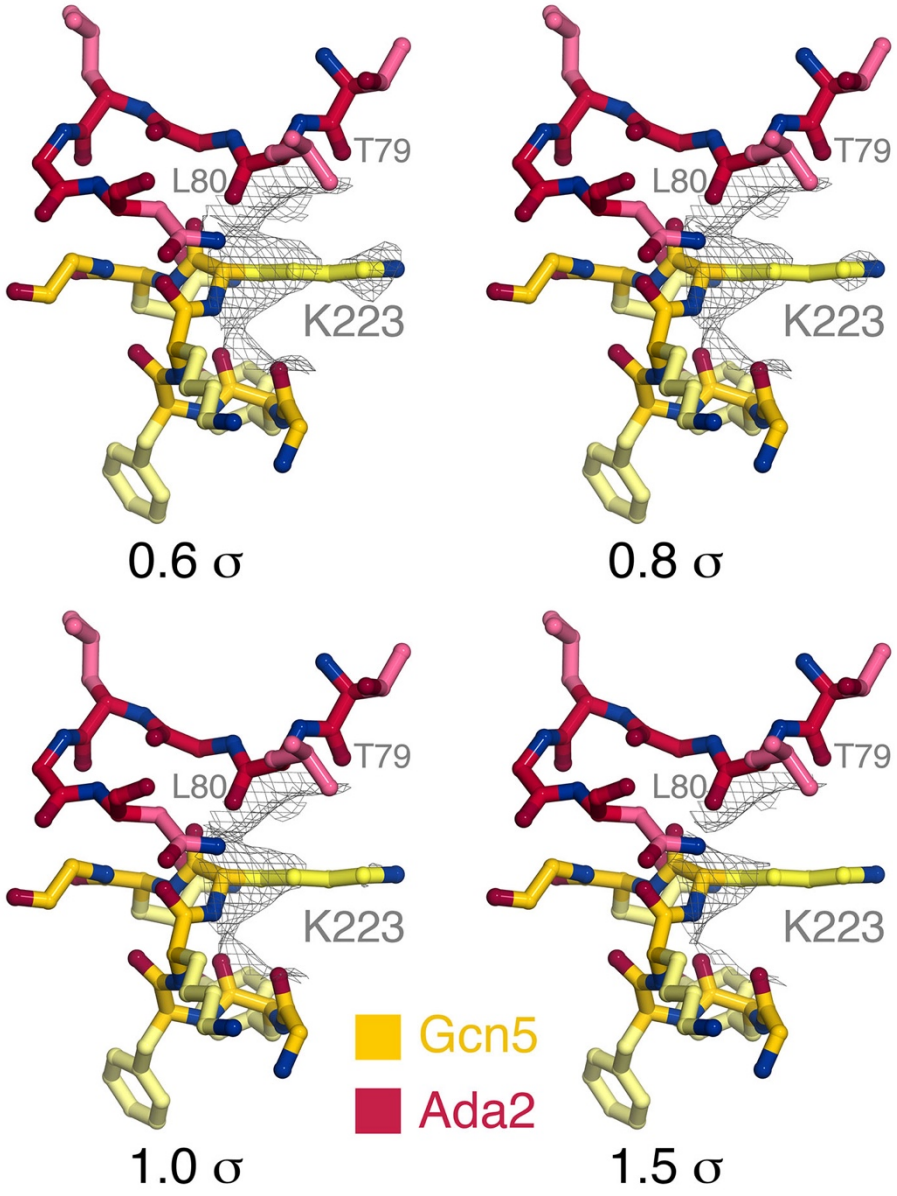

Fig. S6. Simulated annealing omit electron density of Gcn5 Lys223 residue in Ada2/Gcn5 crystal form 1 structure at different map contouring levels. Map calculated using PHENIX crystallographic software.

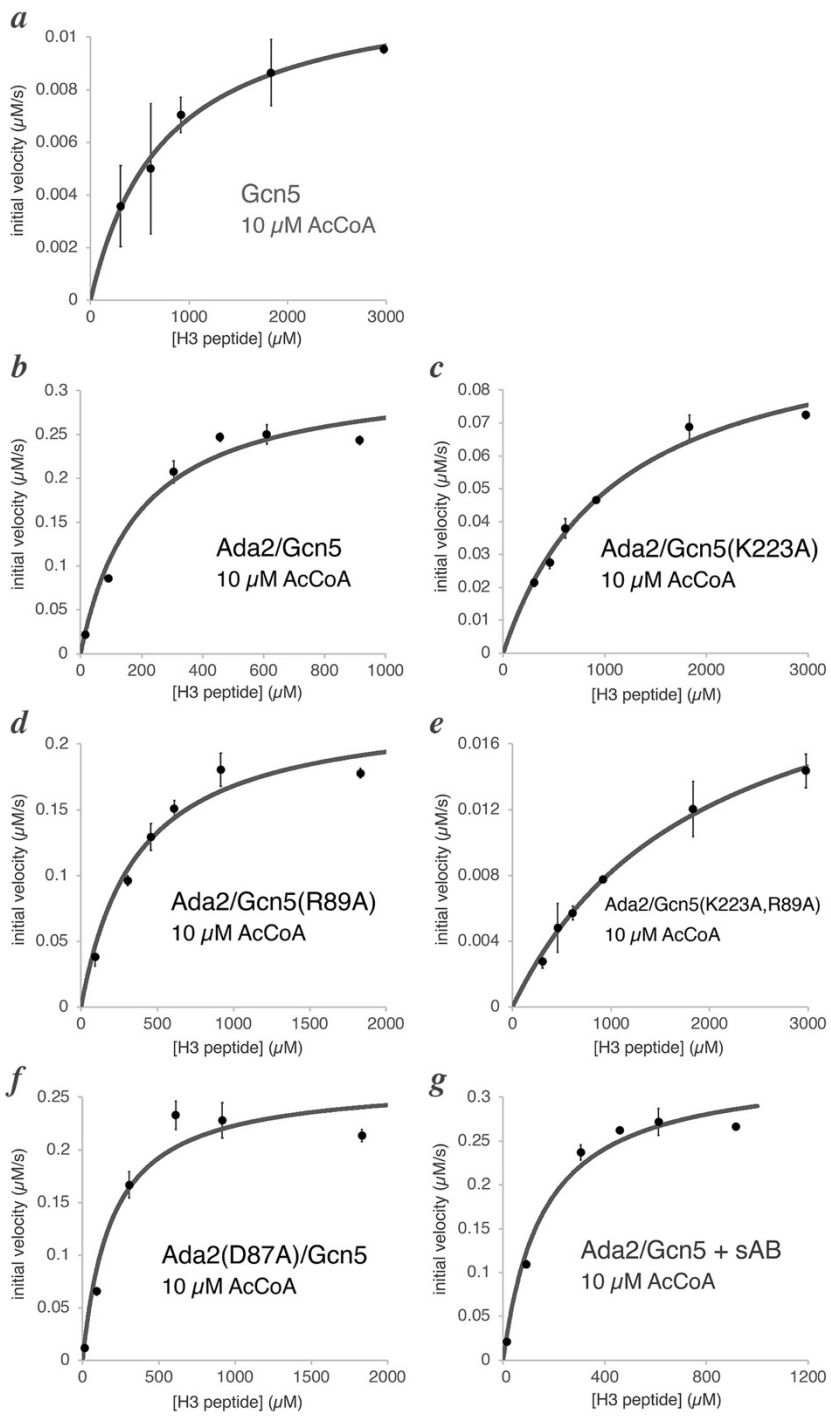

Fig. S7. Histone acetyltransferase assays for Gcn5 and Ada2/Gcn5 complexes in 10 μM acetylCoA. Plots of initial velocity as a function of H3 peptide substrate concentration are shown for (a) Gcn5, (b) Ada2/Gcn5 wild type complex, (c) Ada2/Gcn5(K223A) mutant complex, (d) Ada2/Gcn5(89A), (e) Ada2/Gcn5(K223A,R89A), (f) Ada2(D87A)/Gcn5 and (g) Ada2/Gcn5 wild type complex with the synthetic antibody used for crystal form 1 added.

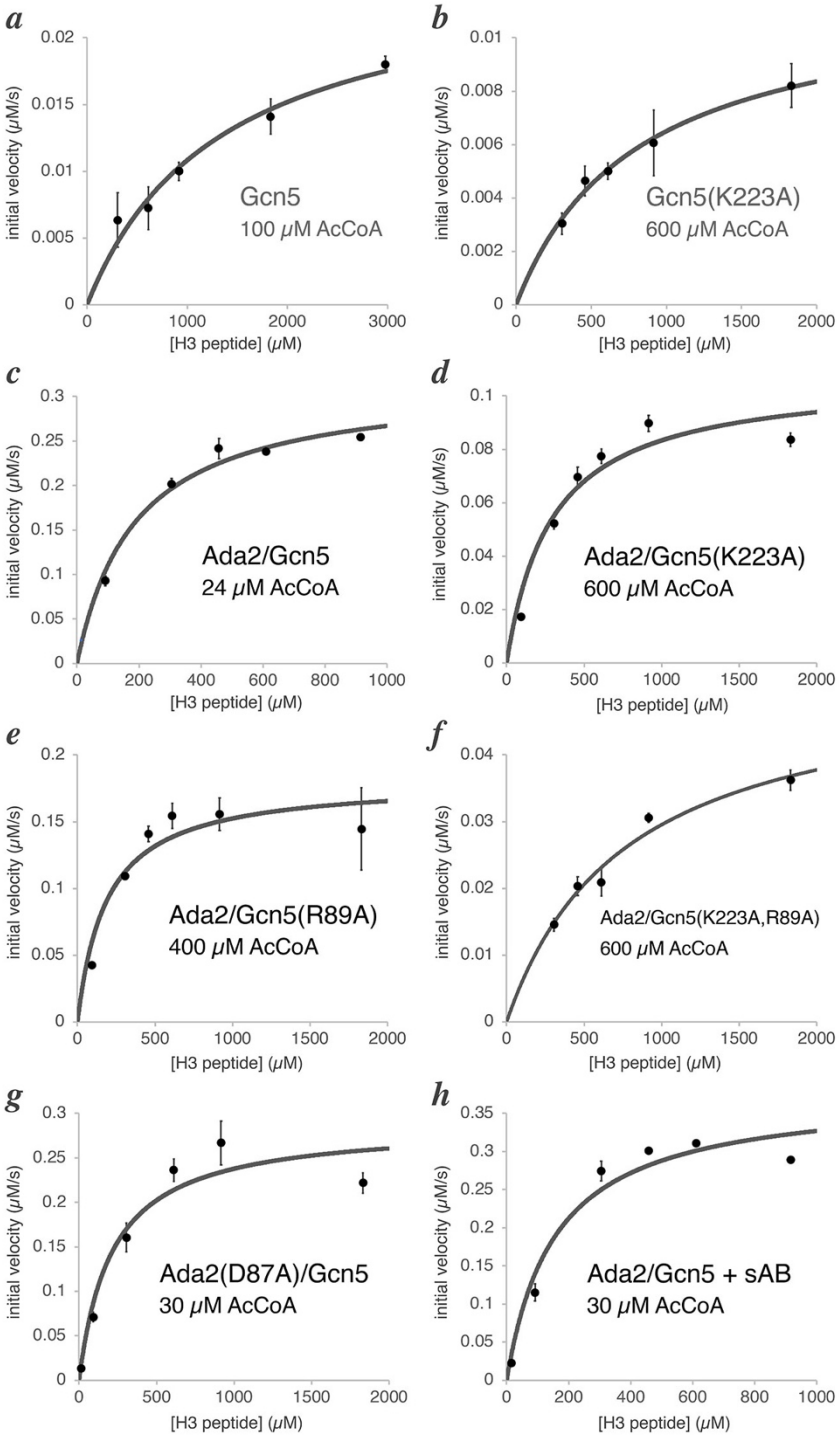

Fig. S8. Histone acetyltransferase assays for Gcn5 and Ada2/Gcn5 complexes in saturating or 600 μM acetyl-CoA. Plots of initial velocity as a function of H3 peptide substrate conc are shown for (a) Gcn5, (b), Gcn5(K223), (c) Ada2/Gcn5 wild type complex, (d) Ada2/Gcn5(K223A) mutant complex, (e) Ada2/Gcn5(89A), (f) Ada2/Gcn5(K223A,R89A), (g) Ada2(D87A)/Gcn5 and (h) Ada2/Gcn5 wild type complex with the synthetic antibody used for crystal form 1 added.

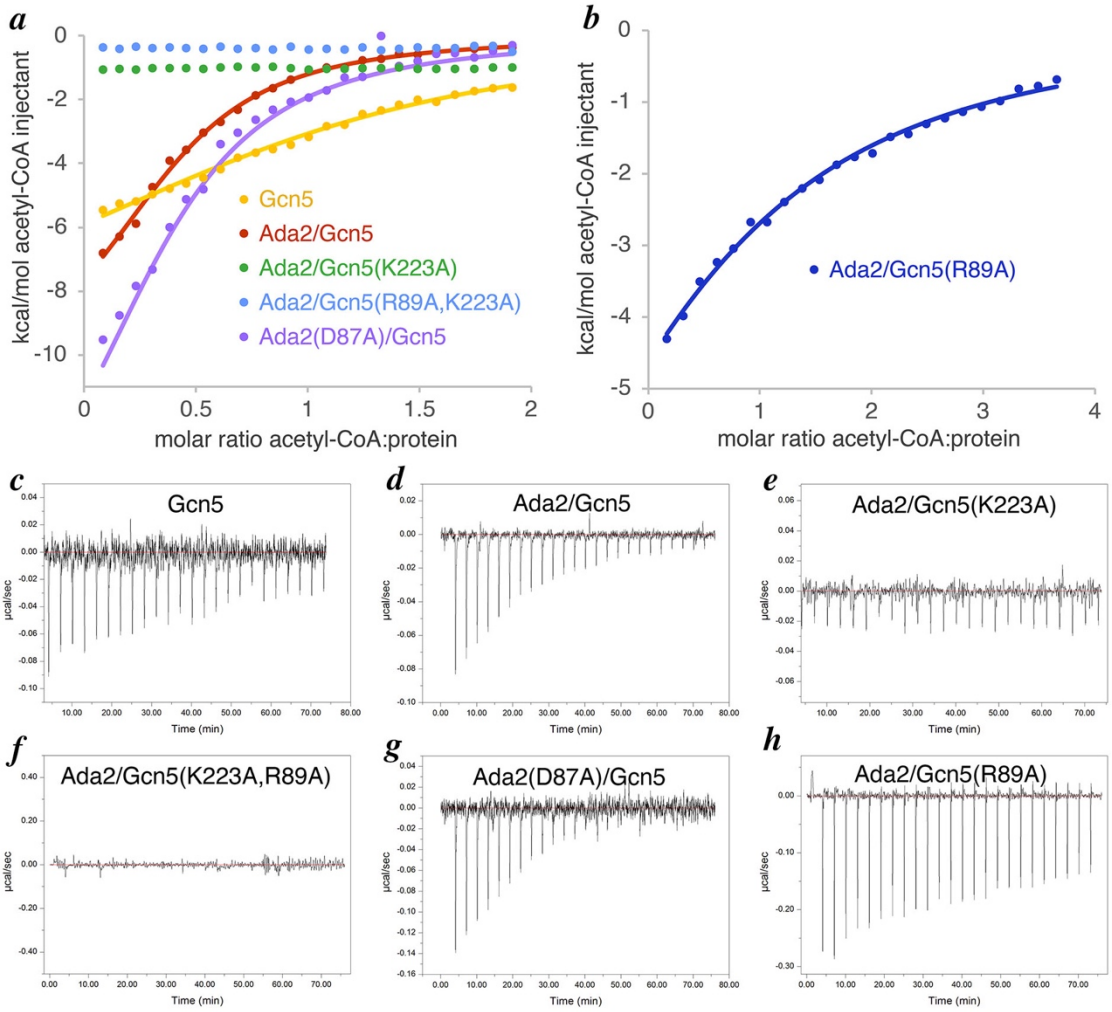

Fig. S9. Isothermal calorimetry plots for acetyl-Coenzyme A (acetyl-CoA) binding to Gcn5 and Ada2/Gcn5 complexes. (a) Plots of heat change upon 100 µM acetyl-CoA injections as a function of acetyl-CoA:protein molar ratio are shown for Gcn5 (yellow), Ada2/Gcn5 (red), Ada2/Gcn5(K223A) (green), Ada2/Gcn5(R89A,K223A) (light blue) and Ada2(D87A)/Gcn5 (purple). (b) Similar plot for Ada2/Gcn5(R89A) (dark blue) using 200 µM acetyl-CoA injections, (c) through (h) Raw calorimetry data for Gcn5, Ada2/Gcn5, Ada2/Gcn5(K223A), Ada2/Gcn5(K223A,R89A), Ada2(D87A)/Gcn5 and Ada2/Gcn5(R89A) respectively.

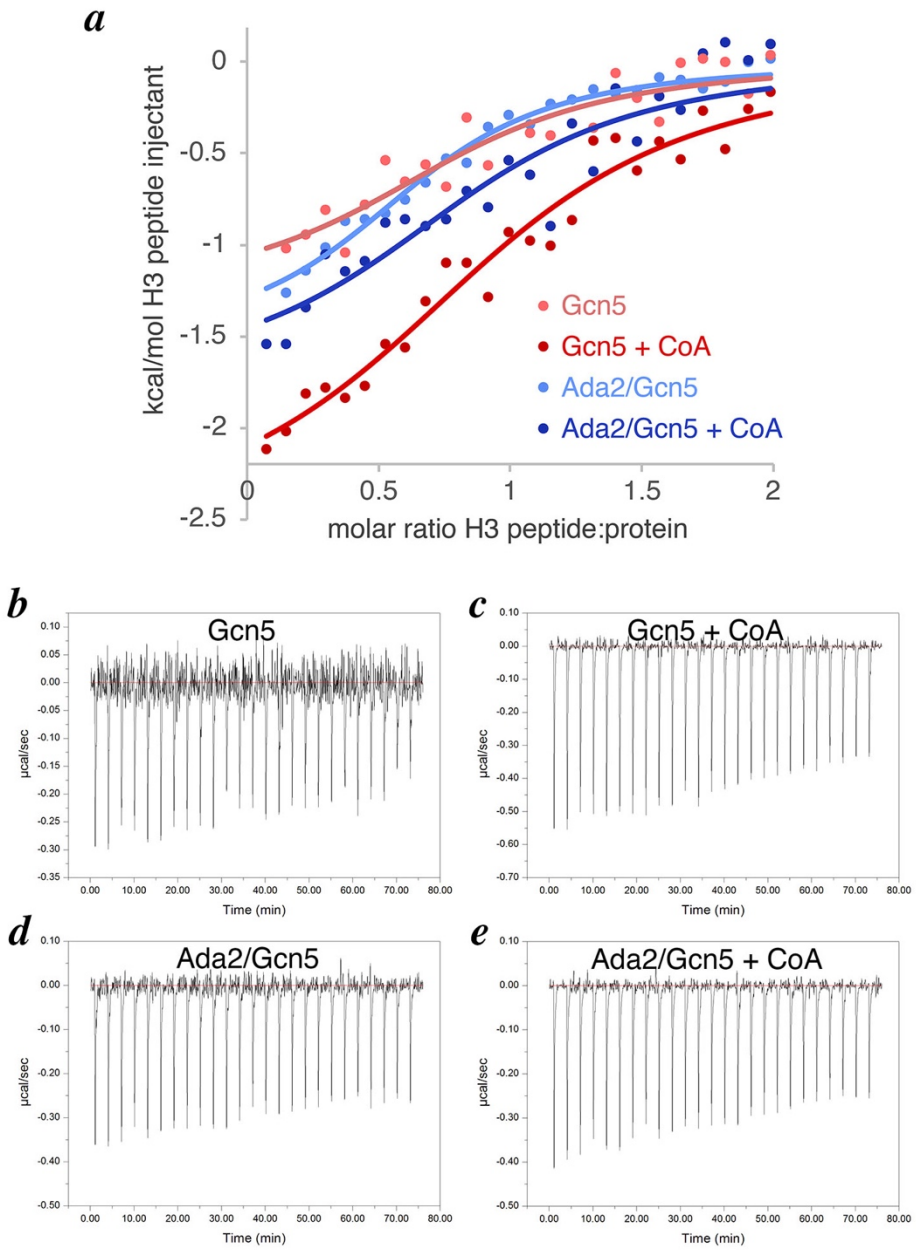

Fig. S10. Isothermal calorimetry plots for histone H3 peptide binding to Gcn5 and Ada2/Gcn5 complexes. (a) Plots of heat change upon 800 µM histone H3(1-20) injections as a function of H3 peptide:protein molar ratio are shown for 80 µM Gcn5 without CoA (pink) or with 80 µM CoA (red), and for 80 µM Ada2/Gcn5 without CoA (light blue) or with 80 µM CoA (blue), (b) through (e) Raw calorimetry data for Gcn5, Gcn5 + CoA, Ada2/Gcn5 and Ada2/Gcn5 + CoA.

a

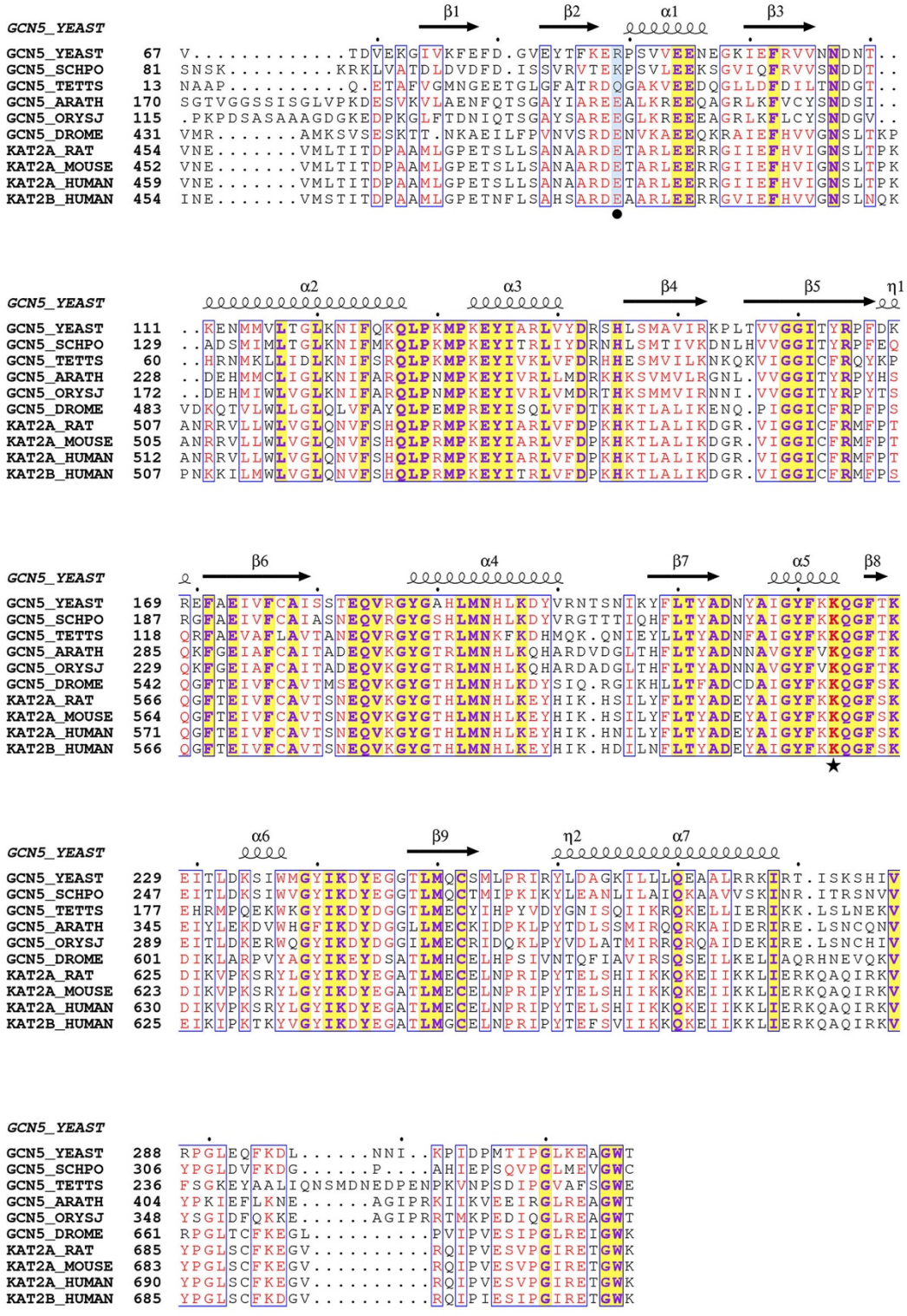
β1 β2 α1 β3
GCN5_YEAST
GCN5_YEAST 67 V.....TDVEKGIVKFEFD.GVEYTFKERPSVVEENEGKIEFRVVNNDNT..
GCN5_SCHPO 81 SNSK.....KRKLVATDLDVDFD.ISSVRVTEKPSVLEEKSGVIQFRVVSNDDT..
GCN5_TETTS 13 NAAP.....Q.ETAFVGMNGEETGLGFATRDQGAKVEEDQGLLDFDILTNDGT..
GCN5_ARATH 170 SGTVGGSSISGLVPKDESVKVLAENFQTSGAYIAREEALKREEQAGRLKFVCYSNDSI..
GCN5_ORYSJ 115 .PKPDSASAAAGDGKEDPKGLFTDNIQTSGAYSAREEGLKREEEAGRLKFLCYSNDGV..
GCN5_DROME 431 VMR.....AMKSVSESKTT.NKAEILFPVNVSRDENVKAEEQKRAIEFHVVGNSLTKP
KAT2A_RAT 454 VNE.....VMLTITDPAAMLGPETSLLSANAARDETARLEERRGIIEFHVIGNSLTPK
KAT2A_MOUSE 452 VNE.....VMLTITDPAAMLGPETSLLSANAARDETARLEERRGIIEFHVIGNSLTPK
KAT2A_HUMAN 459 VNE.....VMLTITDPAAMLGPETSLLSANAARDETARLEERRGIIEFHVIGNSLTPK
KAT2B_HUMAN 454 INE.....VMSTITDPAAMLGPETNFLSAHSARDEAARLEERRGVIEFHVVGNSLNQK
α2 α3 β4 β5 η1
GCN5_YEAST
GCN5_YEAST 111 ..KENMMVLTGLKNIFQKQLPKMPKEYIARLVYDRSHLSMAVIRKPLTVVGGITYRPFDK
GCN5_SCHPO 129 ..ADSMIMLTGLKNIFMKQLPKMPKEYITRLIYDRNHLSMTIVKDNLHVVGGITYRPFEQ
GCN5_TETTS 60 ..HRNMKLLIDLKNIFSRQLPKMPKEYIVKLVFDRHHESMVILKNKQKVIGGICFRQYKP
GCN5_ARATH 228 ..DEHMMCLIGLKNIFARQLPNMPKEYIVRLLMDRKHKSVMVLRGNL.VVGGITYRPYHS
GCN5_ORYSJ 172 ..DEHMIWLVGLKNIFARQLPNMPKEYIVRLVMDRTHKSMMVIRNNI.VVGGITYRPYTS
GCN5_DROME 483 VDKQTVLWLLGLQLVFAYQLPEMPREYISQLVFDTKHKTLALIKENQ.PIGGICFRPFPS
KAT2A_RAT 507 ANRRVLLWLVGLQNVFSHQLPRMPKEYIARLVFDPKHKTLALIKDGR.VIGGICFRMFPT
KAT2A_MOUSE 505 ANRRVLLWLVGLQNVFSHQLPRMPKEYIARLVFDPKHKTLALIKDGR.VIGGICFRMFPT
KAT2A_HUMAN 512 ANRRVLLWLVGLQNVFSHQLPRMPKEYIARLVFDPKHKTLALIKDGR.VIGGICFRMFPT
KAT2B_HUMAN 507 PNKKILMWLVGLQNVFSHQLPRMPKEYITRLVFDPKHKTLALIKDGR.VIGGICFRMFPS
β6 α4 β7 α5 β8
GCN5_YEAST
GCN5_YEAST 169 REFFAEIVFCAISSTEQVRGYGAHLMNHLKDYVRNTSNIKYFLTYADNYAIGYFKKQGFTK
GCN5_SCHPO 187 RGFAEIVFCAIASNEQVRGYGSHLMNHLKDYVRGTTTIQHFLTYADNYAIGYFKKQGFTK
GCN5_TETTS 118 QRFAEVAFLAVTANEQVRGYGTRLMNKFKDHMQK.QNIEYLLTYADNFAIGYFKKQGFTK
GCN5_ARATH 285 QKFGEIAFCAITADEQVKGYGTRLMNHLKQHARDVDGLTHFLTYADNNAVGYFVKQGFTK
GCN5_ORYSJ 229 QKFGEIAFCAITADEQVKGYGTRLMNHLKQHARDADGLTHFLTYADNNAVGYFVKQGFTK
GCN5_DROME 542 QGFTEIVFCAVTMSEQVKGYGTHLMNHLKDYSIQ.RGIKHLLTFADCDAIGYFKKQGFSK
KAT2A_RAT 566 QGFTEIVFCAVTSNEQVKGYGTHLMNHLKEYHIK.HSILYFLTYADEYAIGYFKKQGFSK
KAT2A_MOUSE 564 QGFTEIVFCAVTSNEQVKGYGTHLMNHLKEYHIK.HSILYFLTYADEYAIGYFKKQGFSK
KAT2A_HUMAN 571 QGFTEIVFCAVTSNEQVKGYGTHLMNHLKEYHIK.HNILYFLTYADEYAIGYFKKQGFSK
KAT2B_HUMAN 566 QGFTEIVFCAVTSNEQVKGYGTHLMNHLKEYHIK.HDILNFLTYADEYAIGYFKKQGFSK
α6 β9 η2 α7
GCN5_YEAST
GCN5_YEAST 229 EITLDKSIWMGYIKDYEGGTLMQCSMLPRIRYLDAGKILLLQEAALRRKIRT.ISKSHIV
GCN5_SCHPO 247 EITLDKSIWVGYIKDYEGGTLMQCTMIPKIKYLEANLILAIQKAAVVSKINR.ITRSNVV
GCN5_TETTS 177 EHRMPQEKWKGYIKDYDGGTLMECYIHPYVDYGNISQIIKRQKELLIERIKK.LSLNEKV
GCN5_ARATH 345 EIYLEKDVWHGFIKDYDGGLLMECKIDPKLPYTDLSSMIRQQRKAIDERIRE.LSNCQNV
GCN5_ORYSJ 289 EITLDKERWQGYIKDYDGGILMECRIDQKLPYVDLATMIRRQRQAIDEKIRE.LSNCHIV
GCN5_DROME 601 DIKLARPVYAGYIKEYDSATLMHCELHPSIVNTQFIAVIRSQSEILKELIAQRHNEVQKV
KAT2A_RAT 625 DIKVPKSRYLGYIKDYEGATLMECELNPRIPYTELSHIIKKQKEIIKKLIERKQAQIRKV
KAT2A_MOUSE 623 DIKVPKSRYLGYIKDYEGATLMECELNPRIPYTELSHIIKKQKEIIKKLIERKQAQIRKV
KAT2A_HUMAN 630 DIKVPKSRYLGYIKDYEGATLMECELNPRIPYTELSHIIKKQKEIIKKLIERKQAQIRKV
KAT2B_HUMAN 625 EIKIPKTKYVGYIKDYEGATLMGCELNPRIPYTEFSVIIKKQKEIIKKLIERKQAQIRKV
GCN5_YEAST
GCN5_YEAST 288 RPGLEQFKDL.....NNI..KPIDPMTIPGLKEAGWT
GCN5_SCHPO 306 YPGLDVFKDG.....P....AHIEPSQVPGLMEVGWC
GCN5_TETTS 236 FSGKEYAALIQNSMDNEDPENPKVNPSDIPGVAFSGWE
GCN5_ARATH 404 YPKIEFLKNE.....AGIPRKIIKVEEIRGLREAGWT
GCN5_ORYSJ 348 YSGIDFQKKE.....AGIPRRTMKPEDIQGLREAGWT
GCN5_DROME 661 RPGLTCFKEGL.....PVIPVESIPGLREIGWK
KAT2A_RAT 685 YPGLSCFKEGV.....RQIPVESVPGIRETGWK
KAT2A_MOUSE 683 YPGLSCFKEGV.....RQIPVESVPGIRETGWK
KAT2A_HUMAN 690 YPGLSCFKEGV.....RQIPVESVPGIRETGWK
KAT2B_HUMAN 685 YPGLSCFKDGV.....RQIPIESIPGIRETGWK

b

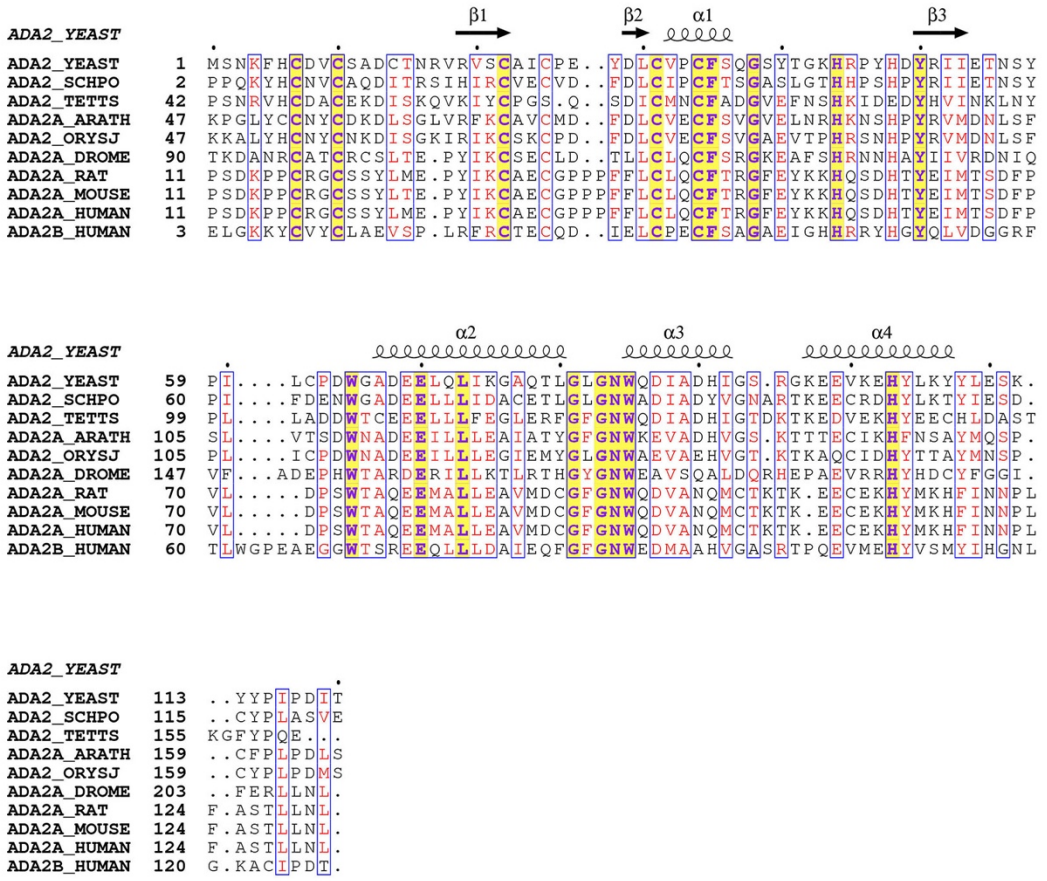

Fig. S11. Sequence alignments of Gcn5 and Ada2 homologs performed using ClustalO (1) and visualized using ESPript (2). Secondary structure elements based on our yeast Ada2/Gcn5 structure are annotated on the top row of the alignment with 3_{10} helices designated as η. Strictly conserved residues are shown in purple on a yellow background. The conserved yeast Gcn5 Lys223 is shown in red on a yellow background and also highlighted with a black star. Gcn5 Arg89 is highlighted with a black dot below the alignment. Only sequences corresponding to yeast Gcn5(67-317) and yeast Ada2(1-120) contained in our crystals are shown.

The sequences aligned (UniProt accession code in parentheses) are:

GCN5_YEAST	*S. cerevisiae*	(Q03330)	ADA2_YEAST	*S. cerevisiae*	(Q02336)
GCN5_SCHPO	*S. pombe*	(Q9UUK2)	ADA2_SCHPO	*S. pombe*	(Q9P7J7)
GCN5_TETTS	*T. thermophila*	(Q245K9)	ADA2_TETTS	*T. thermophila*	(Q24DR4)
GCN5_ARATH	*A. thaliana*	(Q9AR19)	ADA2A_ARATH	*A. thaliana*	(Q9SFD5)
GCN5_ORYSJ	*O. sativa japonica*	(Q338B9)	ADA2_ORYSJ	*O. sativa japonica*	(Q75LL6)
GCN5_DROME	*D. melanogaster*	(Q9VTZ1)	ADA2A_DROME	*D. melanogaster*	(Q7KSD8)
KAT2A_RAT	*R. norvegicus*	(D4ACX5)	ADA2A_RAT	*R. norvegicus*	(Q6AYE3)
KAT2A_MOUSE	*M. musculus*	(Q9JHD2)	ADA2A_MOUSE	*M. musculus*	(Q8CHV6)
KAT2A_HUMAN	*H. sapiens*	(Q92830)	ADA2A_HUMAN	*H. sapiens*	(O75478)
KAT2B_HUMAN	*H. sapiens*	(Q92831)	ADA2B_HUMAN	*H. sapiens*	(Q86TJ2)

Supplementary Table S1: Data collection and refinement statistics

Crystals	Ada2/Gcn5 crystal form 1	Ada2/Gcn5 crystal form 2
PDB code	6CW2	6CW3
Data collection		
Wavelength (Å)	0.9792	0.9792
Space group	$P3_2$ 2 1	$P2_12_12_1$
Cell Dimensions		
a (Å)	191.816	101.657
b (Å)	191.816	104.061
c (Å)	92.674	166.335
α (°)	90	90
β (°)	90	90
γ (°)	120	90
Resolution (Å)	166.1-2.67 (2.75-2.67)[a]	104.06-1.98 (2.01-1.98)
R_{sym} (%)	19.6 (412.7)	6.2 (146.5)
R_{pim} (%)	4.5 (94.7)	2.6 (66.1)
<I/σ>	15.4 (0.8)	16 (1.0)
Redundancy	20.1 (19.9)	6.6 (5.7)
Unique reflection	55876	123142
Completeness (%)	100.0 (100.0)	99.9 (99.9)
Refinement		
Resolution (Å)	95.9-2.67	88.2-1.98
No. reflections	55 713	123 045
R_{work}/R_{free} [b](%)	25.42/28.78	20.25/22.73
r.m.s.d.[c] bonds/angles	0.008/1.747	0.008/1.158
Number of atoms		
Protein	5 909	11 171
Zinc ion	2	4
Water	44	662
B factors		
Protein	87	63.2
ligands	86.4	95.9
Water	69	58.5
Ramachandran		
Favored (%)	92.07	94.80
Allowed (%)	6.08	4.35
Outlier (%)	1.85	0.84

[a]Values in parentheses are those of the highest resolution shell.
[b]Calculated from about 5% of the reflection set aside during refinement
[c]r.m.s.d., root mean square deviation.

Supplementary Table S2: Dissociation constants for Gcn5(67-317) and Ada2(1-120)/Gcn5(67-317) binding to histone H3(1-20) peptide in the absence or presence of coenzyme A

	CoA	Kd
Gcn5	–	15.6 ± 9.4 μM
Gcn5	+	19.2 ± 5.3 μM
Ada2/Gcn5	–	12.2 ± 2.4 μM
Ada2/Gcn5	+	16.2 ± 8.9 μM

References

1. Sievers F, et al. (2011) Fast, scalable generation of high-quality protein multiple sequence alignments using Clustal Omega. *Mol Syst Biol* 7(1):539–539.
2. Robert X, Gouet P (2014) Deciphering key features in protein structures with the new ENDscript server. *Nucleic Acids Res* 42(Web Server issue):W320–4.